PERGAMON

Deep-Sea Research I 47 (2000) 901–936

DEEP-SEA RESEARCH
PART I

Export flux in the western and central equatorial Pacific: zonal and temporal variability

John P. Dunne[a,*], James W. Murray[a], Martine Rodier[b], Dennis A. Hansell[c]

[a]*School of Oceanography, Box 357940, University of Washington, Seattle, WA 98195-7940, USA*
[b]*ORSTOM, Centre d'Ocianologie de Marseille, Station marine d'Endoume, Rue de la Batterie-des-Lions, 13007, Marseille, France*
[c]*Bermuda Biological Station for Research, Inc. St. Georges, GE-01, Bermuda*

Received 21 December 1998; received in revised form 10 August 1999; accepted 1 September 1999

Abstract

Particulate organic carbon export fluxes were measured along the equator to resolve the zonal extent of high productivity in the equatorial Pacific during two cruises: the French JGOFS FLUPAC study aboard the R/V *l'Atalante* in October 1994 and the Zonal Flux study aboard the R/V *Thomas G. Thompson* in April 1996. Both cruise tracks went along the equator from 165°E to 150°W. The cruises took place under different seasonal and El Niño-Southern Oscillation (ENSO) conditions: FLUPAC during a strong El Niño in the boreal fall and Zonal Flux during a mild La Niña in the boreal spring. Drifting sediment traps were deployed at the base of the euphotic zone and calibrated using ^{234}Th. These traps showed over-trapping by 2.7 ± 1.5 times during FLUPAC and 1.5 ± 0.7 times during Zonal Flux. During the FLUPAC time-series at 167°E, the upper euphotic zone was devoid of nitrate, and particulate organic carbon export was low (6 ± 1 mmol m^{-2} d^{-1}). The FLUPAC time-series at 150°W had abundant nitrate and much higher particulate organic carbon export (12 ± 1 mmol m^{-2} d^{-1}). Similarly high levels of particulate organic carbon export were observed all along the equator during the Zonal Flux cruise (10 ± 2 mmol m^{-2} d^{-1}), when cold tongue, high nitrate conditions extended west of 165°E.

Synthesis of this data with results from the US Joint Global Ocean Flux Study (JGOFS) equatorial Pacific (EqPac) program allowed a detailed evaluation of equatorial production variability. Data from the TOGA-TAO array illustrated that both Kelvin Waves and tropical instability waves (TIW) were present during the FLUPAC cruise, while neither wave type was present during Zonal Flux. Comparison with results from the US JGOFS EqPac cruises

* Corresponding author. Tel.: 001-206-221-5630; fax: 001-206-685-3351.
E-mail address: jdunne@ocean.washington.edu (J.P. Dunne)

0967-0637/00/$ - see front matter
PII: S0967-0637(99)00089-8

suggested that the ubiquity of super-μM nitrate was the major forcing for new production and particle export near the equator, accounting for a doubling of production over areas with only subsurface nitrate. Within the high nitrate zone, new production and particle export were both found to be enhanced during TIW activity and diminished during Kelvin Wave activity. While the geographical extent of surface nutrients and associated enhanced production is clearly a strong function of season and ENSO, we suggest that equatorially trapped waves — rather than long-term variability in upwelling velocity — are the dominant sources of variability within the equatorial upwelling zone. Comparison of new production and particle export and regressions between nitrate and total organic carbon (TOC) suggest that accumulation and transport of TOC accounts for 17–27% of new production.

1. Introduction

New and export production from the equatorial Pacific upwelling zone are important moderators of variability in the ocean carbon cycle. Chavez and Barber (1987) suggested that the Wyrtki box (90°E–180°E, 5°N–5°S), which corresponds to 3% of the global ocean area, contributes from 18 to 56% of global new production (more recently revised to 26%; Chavez and Toggweiler, 1995). Barber and Kogelschatz (1990) suggested that the El Niño-Southern Oscillation (ENSO), through modulation of the east–west tilt of the equatorial nitracline, was a primary source of new production variability, reducing new production in the eastern Pacific and increasing it in the western Pacific during El Nino. Though a great deal has been learned since then about meridional and temporal variability in the central equatorial Pacific, little more is known about the gradient in export production between the eastern and western equatorial Pacific or about the relative roles of equatorially trapped waves, season and ENSO in modulating new and export production.

Much of what we know about the equatorial Pacific comes from the US Joint Global Ocean Flux Study (JGOFS-EqPac), which set out to better characterize carbon fluxes in the high-nitrate low-chlorophyll (HNLC) region of the central and eastern equatorial Pacific (e.g. Murray et al., 1994). The EqPac study found that small phytoplankton (Bidigare and Ondrusek, 1996) were recycled by microzooplankton (Landry et al., 1995) in an efficient microbial loop. Primary production was largely based on recycled nutrients (Barber et al., 1996; McCarthy et al., 1996), and the particle export flux was low (Buesseler et al., 1995; Murray et al., 1996; Bacon et al., 1996). A great deal of temporal variability was observed. Between boreal spring, El Niño conditions of Survey I, and boreal fall, non-El Niño conditions of Survey II, surface nitrate concentrations and primary production doubled (3–6 μM, 62 to 112 mmol m^{-2} d^{-1}, respectively; Barber et al., 1995) and mesozooplankton grazing quadrupled (5 to 24 mmol m^{-2} d^{-1}; Dam et al., 1995) while the inventory of particulate organic carbon increased by only 20% within the equatorial upwelling region of 2°N–2°S. While studies based on ^{234}Th and in situ filtered C : Th ratios found only a slight difference in particulate organic carbon (POC) export between time periods (Buesseler et al., 1995; Bacon et al., 1996), POC export from ^{234}Th calibrated sediment

traps also doubled (5 to 12 mmol m^{-2} d^{-1}; Murray et al., 1996). Synthesis of EqPac data showed that the HNLC condition persisted due to intense grazing control of small phytoplankton and iron limitation of large phytoplankton (Landry et al., 1997). Seasonal variability in biomass and production was accurately modeled as a response to variability in upwelled iron (Loukos et al., 1997).

One of the issues that remained unresolved after EqPac was the zonal extent of the high nitrate, highly productive central equatorial Pacific with respect to its transition to the western Pacific, a region devoid of nitrate in the upper euphotic zone (see review by Barber and Kogelschatz, 1990). The extent to which particle export varies zonally is of great importance for global oceanic uptake of carbon dioxide. Primary production in the western equatorial Pacific (155°E, 10°N–10°S) during the Australian JGOFS program varied over a considerable range, 20–50 mmol C m^{-2} d^{-1} (Mackey et al., 1997). Particulate organic carbon export in this region has never been reported. If the western equatorial Pacific were to resemble oligotrophic gyres it would have primary production less than 35 mmol C m^{-2} d^{-1} with particulate organic carbon export of about 2 mmol C m^{-2} d^{-1} (Michaels et al., 1994; Karl et al., 1996) and total export production about 5 mmol C m^{-2} d^{-1} (Emerson et al., 1997). If this condition applies to the western equatorial Pacific, it would imply a large zonal gradient in particle flux along the equator.

Another issue not resolved by EqPac was separation of seasonal, El Niño-Southern Oscillation (ENSO) and wave-induced variability as forcing functions on equatorial biogeochemistry. Primary production (Barber et al., 1995), new production (McCarthy et al., 1996), microzooplankton grazing (Landry et al., 1995), mesozooplankton grazing (Dam et al., 1995) and POC export (Murray et al., 1996; Bacon et al., 1996) were all found to vary significantly between the boreal spring, El Niño Survey I/Time-series I and the boreal fall Survey II/Time-series II. These differences may have been associated with seasonal increases in wind-driven upwelling during the boreal fall Survey II/Time-series II, inter-annual variability due to the strong El Niño condition during the Survey/Time-series I period, Kelvin waves during Survey I/Time-series I or tropical instability waves during Survey II/Time-series II. Analysis of only the two time periods was not enough to distinguish between these effects and ascertain which were the dominant sources of variability.

^{234}Th was extensively used to estimate particle export during the EqPac program (Buesseler et al., 1995; Murray et al., 1996; Bacon et al., 1996). The most basic particle-^{234}Th cycling model (Bacon and Anderson, 1982) is a steady-state mass balance in which the vertical flux of ^{234}Th equals the difference between the rates of in-situ production of ^{234}Th ($t_{1/2} = 24.1$ days) from its long-lived, conservative parent ^{238}U ($t_{1/2} = 4.47 \times 10^9$ yr) and in situ radioactive decay of ^{234}Th. The relationship between this calculation of ^{234}Th flux and the export flux of organic carbon depends on the mechanisms of particle cycling and on the organic carbon to ^{234}Th ratio of sinking particles. The ^{234}Th method consists of two parts: (1) estimation of the ^{234}Th sinking flux by measurement of the radioactive deficiency of ^{234}Th from its parent, ^{238}U, and any spatial or temporal gradients in ^{234}Th and (2) estimation of the ^{234}Th and carbon content of sinking particles to convert the ^{234}Th flux to a carbon flux.

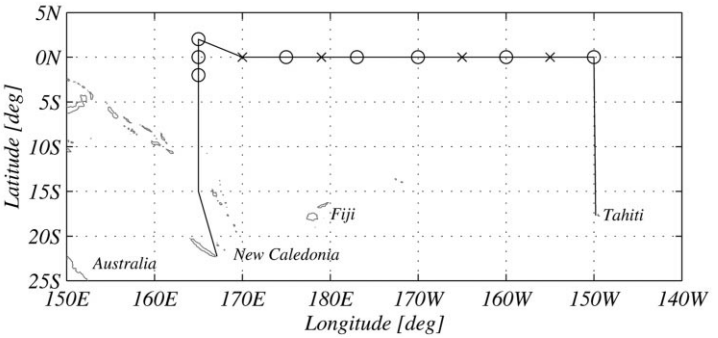

Fig. 1. Map of the equatorial Pacific showing the cruise track for the Zonal Flux cruises with circles showing stations of 2-day trap deployments. The FLUPAC cruise track was similar to that during Zonal Flux with triplicate 2-day trap deployments at 167°E and 150°W.

The purpose of this paper is to present results from two zonal transect cruises along the equator between 165°E and 150°W: the French JGOFS FLUPAC study aboard the R/V *l'Atalante* in October, 1994 and the Zonal Flux study aboard the R/V *Thomas G. Thompson* in April, 1996. Both cruise tracks went from New Caledonia to Tahiti (Fig. 1). These cruises took place under extremely different conditions: FLUPAC during a strong El Niño and Zonal Flux during a mild La Niña. FLUPAC included intensive 7-day time-series studies of the two endpoints while Zonal Flux included an extensive study at six two-day stations along the equator. The goals of this study were fourfold: (1) to measure zonal gradients in carbon fluxes in order to determine how far the zone of high productivity in the central equatorial Pacific extends toward the west, (2) to distinguish the sources of temporal variability of particle export in the equatorial upwelling zone through comparison with results from EqPac, and (3) to describe the role of total organic carbon accumulation and transport as a sink for new production.

2. Samples and methods

The FLUPAC cruise occupied two six-day time-series stations at the equator, one at 167°E (TS-I) and another at 150°W (TS-II) aboard the R/V *l'Atalante* in October 1994. The Zonal Flux cruise occupied two-day stations at 2°S, 0° and 2°N at 165°E and along the equator at 174°E, 177°W, 170°W, 160°W and 150°W aboard the R/V *Thompson* in April–May 1996. Samples were collected for complete sets of hydrographic, chemical and biological parameters at each station. Results for the FLUPAC cruise are described in Rodier and Le Borgne (1997) and are published in two data volumes (Le Borgne et al., 1995; Le Borgne and Gesbert, 1995).

Water column samples for total ^{234}Th were collected using an integrating sampling method from the surface to the intended sediment trap depths using CTD-rosette

mounted 10-l Niskin bottles in which equal volume samples were collected at an even 10–20 m depth spacing and combined into a single ~18-l sample (after Buesseler et al., 1994). A large volume, narrow-mouthed bottle was used to minimize uncertainty in volume to 0.2%. Sampling was performed daily during each of the FLUPAC time series and once per station during Zonal Flux. Short, 4 h stations were conducted every 2° long the equator during FLUPAC and every three to five degrees along the equator during Zonal Flux. Twice during Zonal Flux, discrete profiles of ^{234}Th were taken in the upper 200 m. Analyses of ^{234}Th were conducted following the combination of the procedures of Anderson and Fleer (1982) and Coale and Bruland (1985) given in Murray et al. (1996). The parent ^{238}U was separated from ^{234}Th within two days aboard ship. Further purification, plating, and beta and alpha counting were performed in Seattle. ^{234}Th activities were decay-corrected to the time of collection (Appendix A). During both cruises, the ^{234}Th standard was calibrated using deep (500–1000 m) samples assumed to be in equilibrium with ^{238}U and proportional to salinity. We used the relationship of (^{238}U dpm/l $= 0.0686 * \sigma_t$) obtained from the work of Ku et al. (1977) and Chen et al. (1986).

Uncertainty in water column samples during FLUPAC were minimized using beta recounting (Buesseler et al., 1994). Background activities on the beta counters for FLUPAC samples were about 0.3 counts per minute, and the efficiency was about 60%. Samples were beta-counted five times over two months. Regression analysis was then used to obtain a more precise estimate of the original activity than possible through single counting. Alpha counting to determine the activity of the ^{230}Th yield tracer had negligible backgrounds and efficiencies of about 33%. Uncertainty (1σ) in the activity of ^{234}Th was estimated from least-squares propagation from the alpha counting uncertainty (2.5% from multiple counting periods), the beta counting regression uncertainty (average 2.6%) and the deep calibration uncertainty (1.4%) combining for a total uncertainty of 4.0% (Appendix A).

Uncertainty in beta counting of Zonal Flux samples was higher and more variable due to three analytical problems: (1) a blockage in the gas line by dust led to variability in carrier gas flow rate; (2) beta counters were unintentionally contaminated by high ^{232}Th samples being measured at the same time; and (3) the increased number of samples prevented multiple beta countings. Factors (1) and (2) resulted in variably elevated background levels. We used weekly checks on counter background activities to constrain the uncertainty. In addition, three criteria were used for rejecting individual countings: counting performed less than three days after a ^{232}Th counting, ^{234}Th counts less than twice background and ^{232}Th counts more than half ^{234}Th counts. Uncertainty in the activity of ^{234}Th from the least-squares propagation including the alpha and calibration uncertainties along with increased beta uncertainty from blanks, efficiencies and single counting gave an average uncertainty of 9.6% (Appendix A).

Sinking particles were sampled using drifting sediment traps as described in Murray et al. (1996). Knauer et al. (1979) style particle interceptor traps (PIT) were used for ^{234}Th and mass. These PITs were cylinders constructed of clear plastic with an inner

diameter of 7.1 cm, an aspect ratio of 8 : 1 (length : diameter) and a baffling system of 1 cm diameter, 10 cm deep tubes. Rodier and Le Borgne, 1997 (Lorenzen et al., 1983) traps were used for carbon and mass. These Lorenzen traps were cylinders constructed of opaque plastic with an inner diameter of 8.0 cm, an aspect ratio of 6.5 : 1 (length : diameter), a 1 cm deep honeycomb baffling system and an automatic closing mechanism. PITs were attached to the Lorenzen trap arrays. Traps were deployed at the base of the euphotic zone at 105–125 m during FLUPAC and at 120–140 m during Zonal Flux. A continuously recording pressure sensor was attached to each trap array to monitor the actual depth. Mesozooplankton swimmers were carefully picked from all trap samples using forceps under the supervision of R. Le Borgne, first by naked eye, then under magnification, then again by naked eye. The swimmer component at FLUPAC TS I was small, averaging less than 5% of total mass. The FLUPAC TS-II site had a larger swimmer component. Total salt-corrected mass (swimmer-free) from three deployments of traps at 100 m and 160 m was 131 mg. Euphausiids and copepods removed from these traps weighed a total of 13 mg. Two large (2.5 cm) Caridae shrimp weighing a total 42 mg were also removed from the second FLUPAC TS-II trap deployment. Had swimmers not been picked, they would have contributed 42% to the total mass. Lorenzen trap filters were picked of foraminifera while PIT style trap filters were not. To account for inter-trap variability in the total amount of material being analyzed, carbon and ^{234}Th data were normalized to mass for direct comparison.

Results for temperature, salinity, nutrients, chlorophyll, and particulate organic carbon (Rodier and Le Borgne, 1997) were obtained from bottles on the ship's rosette using JGOFS protocols. ^{14}C primary production (A. Le Bouteiller and Z. Johnson, personal communication) and ^{15}N new production (C. Navarette, 1998; Aufdenkampe et al., submitted) were obtained through 6 h in situ incubations of bottle samples using JGOFS protocols. FLUPAC data are available in two data volumes (LeBorgne et al., 1995a,b). Samples were taken for total organic carbon on both cruises. Data and interpretation for the FLUPAC cruise were given in Hansell et al. (1997b). Analyses for TOC from the Zonal Flux cruise were made at the Bermuda Biological Station using the same method (Hansell et al., 1997b).

In this study we estimated upwelling velocities to correct the model ^{234}Th sinking flux for advection. Horizontal velocities were obtained from the general circulation model of the National Centers for Environmental Prediction Pacific Ocean Hindcast Model. This model assimilates TOGA-TAO temperature and TOPEX/Poseidon sea surface height data to infer circulation on a horizontal resolution of 1° latitude by 1.5° longitude and a vertical resolution of 15 grid points in the upper 200 m (http://nic.fb4.noaa.gov:8000/research/cmb/climate_ocnanl.html). Vertical velocities were then estimated from divergence in horizontal velocities. We used temperature, dynamic height and meridional velocity data from the TOGA-TAO array and data on the Southern Oscillation Index (SOI), all courtesy of the National Oceanic and Atmospheric Administration (http://www.pmel.noaa.gov/toga-tao/home.html). All data can be found at the US Joint Global Ocean Flux Study home page (http://www1.whoi.edu/jgofs.html).

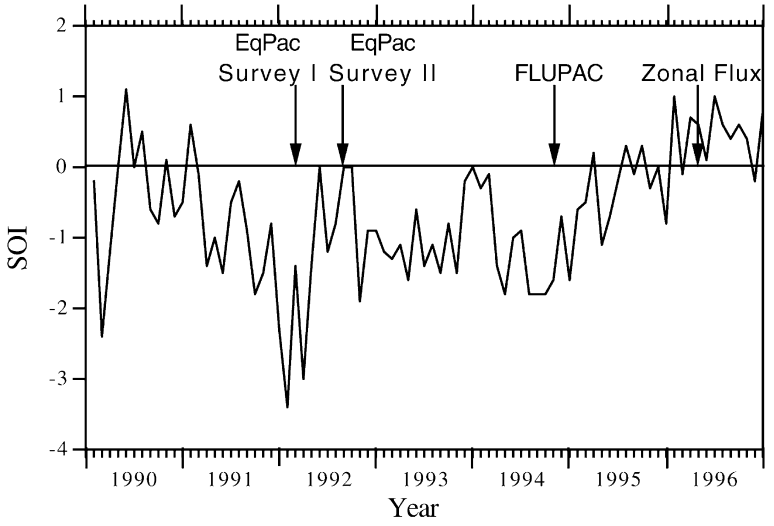

Fig. 2. Southern Oscillation Index for the years 1990 through 1996 (courtesy National Oceanic and Atmospheric Administration).

3. Results

3.1. Hydrography, nutrients, biomass and productivity

The western Pacific warm pool was well established in October, 1994, as a result of El Niño conditions present almost continuously from late 1991 through early 1995 (Fig. 2). The Southern Oscillation Index (SOI) averaged -1.7 for the three months before the FLUPAC cruise, indicating particularly strong El Niño conditions. Conditions during the Zonal Flux cruise were drastically different. The SOI averaged $+0.5$ for the three months before the Zonal Flux cruise, indicating moderate La Niña conditions.

Temperature and salinity for both zonal transects are shown in Fig. 3. FLUPAC surface waters were 29–31°C in the warm pool. The warmest waters were centered near the date line, but 29°C water extended eastward all the way to 167°W. A strong thermocline was established at 100 m across the entire transect. Temperatures were much lower during Zonal Flux with the warm pool (defined by the 29°C isotherm) shifted over 37° westward relative to FLUPAC. Isotherms shoaled towards the east approximately 1 m/degree over 45° of longitude with the thermocline much shallower and more intense in the east. During FLUPAC the western equatorial Pacific warm pool was characteristically low in salinity ($S = 34$) with isohalines rising eastward from the base of the euphotic zone at 165°E to the surface near 175°W. During Zonal Flux, salinity was everywhere higher in the western Pacific than during FLUPAC, consistent with the lack of a warm pool at 165°E. During FLUPAC TS-I, variability

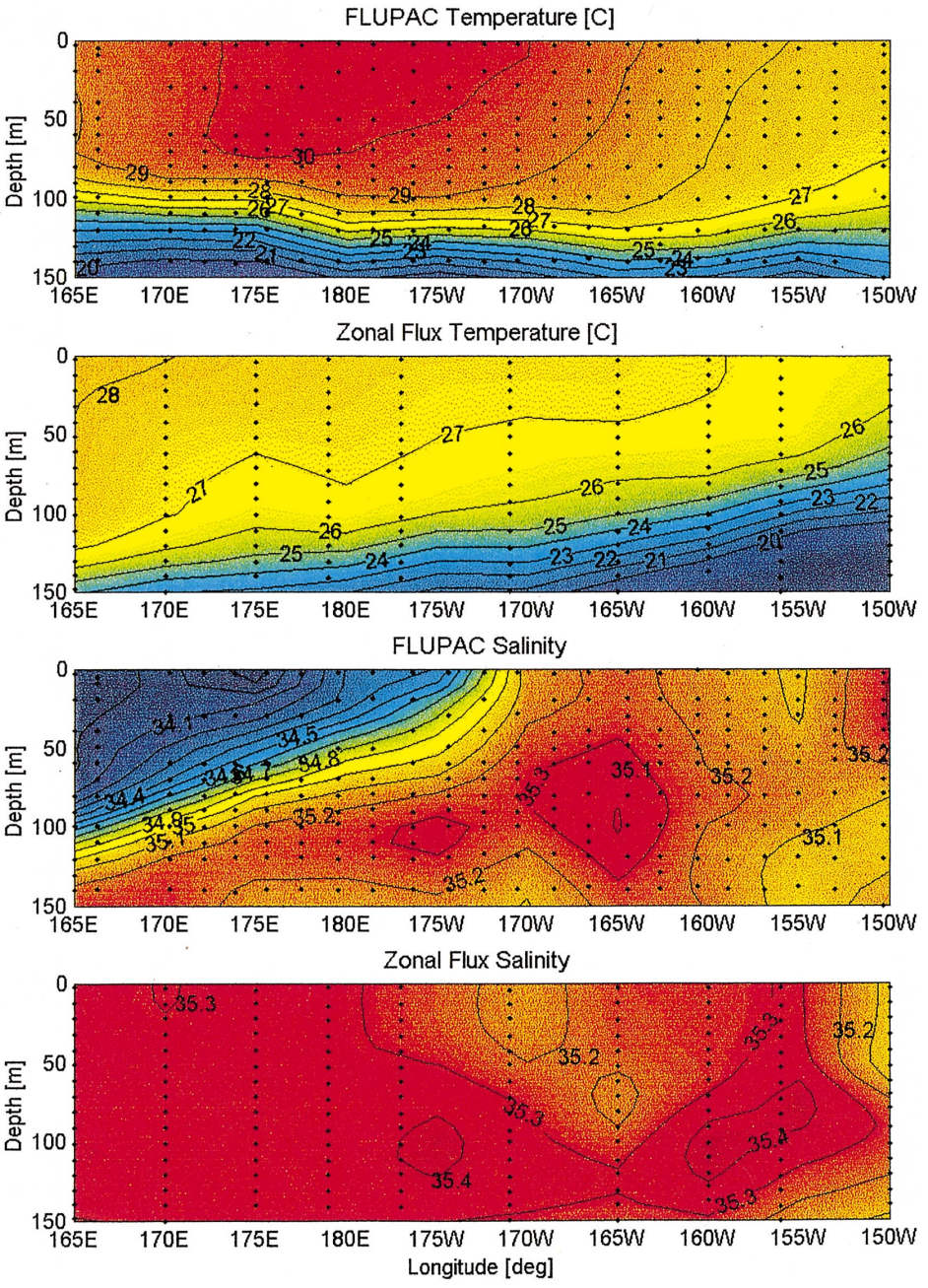

Fig. 3. Longitude versus depth contours for temperature and salinity from the FLUPAC and Zonal Flux cruises.

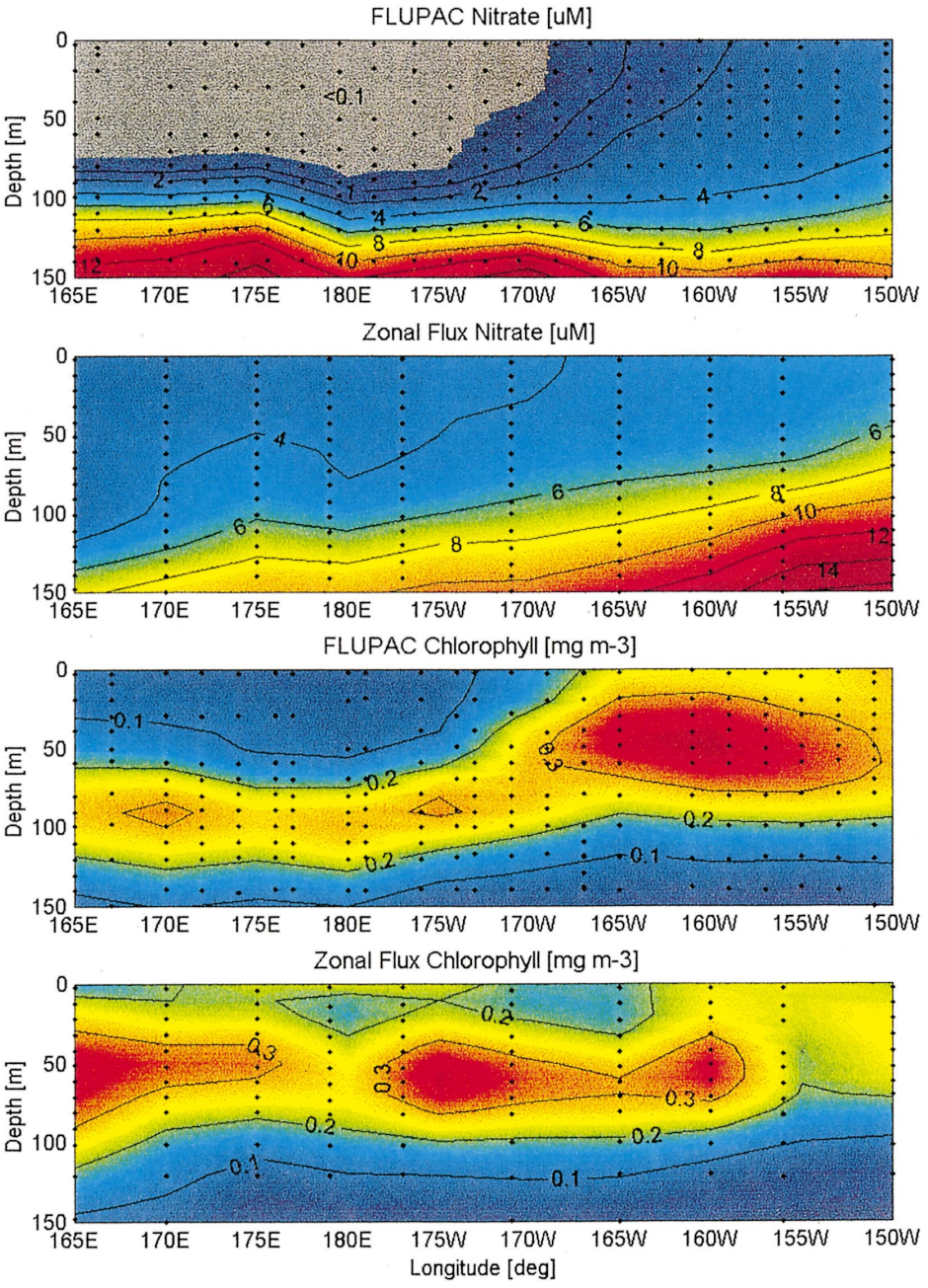

Fig. 4. Longitude versus depth contours for nitrate (μM) and chlorophyll *a* (mg m^{-3}) from the FLUPAC and Zonal Flux cruises.

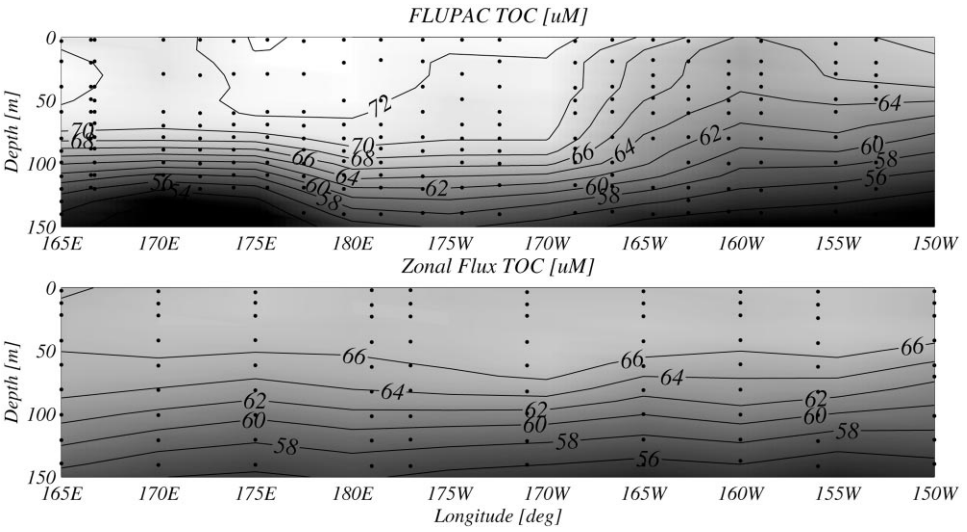

Fig. 5. Longitude versus depth contours for total organic carbon (TOC; μM) during the FLUPAC and Zonal Flux cruises.

in salinity of the warm pool determined variability in mixed layer depths, which averaged 57 ± 32 m by the density criterion $\Delta\rho_{0\text{-MLD}} > 0.125$ (Gardner et al., 1995). Elsewhere, temperature determined the mixed layer depth, which was deep at FLUPAC TS-II (91 ± 13 m) and shallow along the entire Zonal Flux transect (49 ± 15 m).

Nitrate and chlorophyll *a* for both zonal transects are shown in Fig. 4. The warm pool was well defined by zero nitrate in the upper euphotic zone during FLUPAC. Elsewhere during both cruises, nitrate followed temperature ($r^2 = 0.93$; Fig. 3). During Zonal Flux surface nitrate was almost 3 μM at 165°E and increased evenly towards the east. Chlorophyll *a* distributions followed similar patterns as nitrate with low surface values during FLUPAC in the warm pool. During FLUPAC there was a deep chlorophyll maximum at 80–100 m in the western equatorial Pacific, which thickened and shoaled to 20–70 m in the east. During Zonal Flux chlorophyll *a* distributions had a subsurface maximum between 30 and 70 m with no zonal trend.

Total organic carbon (TOC) distributions from both zonal transects are shown in Fig. 5. As described in Hansell et al. (1997), high values of TOC during FLUPAC were observed in the warm pool, with a strong front at 170°W and a strong, inverse relationship with nitrate ($r^2 = 0.78$). Observations of TOC during Zonal Flux were in agreement with the rest of the observations, demonstrating only minimal zonal gradients and following the same relationship observed between nitrate and TOC during FLUPAC.

Primary productivity was relatively low in the warm pool at FLUPAC TS-I, 52 ± 3 mmol C m^{-2} d^{-1}, while in the upwelling zone at FLUPAC TS-II, primary

production was higher, 94 ± 3 mmol C m^{-2} d^{-1} (Rodier and Le Borgne, 1997). During Zonal Flux primary production was relatively constant over the entire equatorial transect from 165°E to 150°W at an intermediate level of 80 ± 7 mmol C m^{-2} d^{-1} (Le Borgne et al., 1999; Z. Johnson, personal communication).

$^{15}NO_3$ new production measured from the surface to the 0.1% light level (~120 m) during FLUPAC was 1.4 mmol N m^{-2} day^{-1} at TS-I and 2.1 mmol N m^{-2} day^{-1} at TS-II (C. Navarette, personal communication; Rodier and Le Borgne, 1997). New production during Zonal Flux was a relatively low 1.0 mmol N m^{-2} day^{-1} at 165°E and increased steadily to 4.8 mmol N m^{-2} day^{-1} at 150°W (Aufdenkampe et al., submitted).

3.1.1. ^{234}Th *activities*

^{234}Th activities as a function of depth are shown for both cruises in Fig. 6. At FLUPAC TS-I ^{234}Th activities were slightly deficient relative to ^{238}U in the upper 110 m (2.16 ± 0.10 dpm/l), in equilibrium with ^{238}U between 100 and 160 m (2.56 ± 0.13 dpm/l) and in slight excess of ^{238}U between 160 m and 210 m (2.64 ± 0.13 dpm/l). At FLUPAC TS-II ^{234}Th activities were more strongly and variably deficient from ^{238}U in the upper 100 m (2.03 ± 0.20 dpm/l) but again in equilibrium with ^{238}U between 100 and 160 m (2.46 ± 0.09 dpm/l) and in slight excess of ^{238}U between 160 m and 210 m (2.69 ± 0.10 dpm/l). One 0–100 m ^{234}Th sample at FLUPAC TS-II was taken a day after the last 2-day trap deployment south of the trap recovery (0.5°S). Though no particulate organic carbon or chlorophyll anomalies were observed in this cast, euphotic zone nitrate values were deficient relative to temperature — evidence that a period of high export from this water mass had recently occurred. We suggest that this water mass was part of an approaching Tropical Instability Wave (see discussion) and do not include the ^{234}Th sample in the deficiency model.

During the Zonal Flux transect remarkably invariant ^{234}Th activities were observed in the upper 120 m (2.02 ± 0.316 dpm/l) with deeper ^{234}Th activities in equilibrium with ^{238}U between 120 and 200 m (2.47 ± 0.13 dpm/l). During Zonal Flux, discrete profiles of ^{234}Th were also obtained at 170°E and 155°W. ^{234}Th activities increased roughly linearly from the surface to 100 m in these profiles with a slight excess of ^{234}Th over ^{238}U below 100 m. Given the relatively high uncertainty in data from the Zonal Flux cruise (~11%), we do not consider the depth dependency of these profiles significantly different and have averaged them to obtain a single ^{234}Th depth dependency in our advection calculations for both cruises.

3.1.2. *Sediment trap fluxes*

Sediment trap fluxes are shown in Fig. 7. In this analysis, we have aggregated the sediment trap data originally collected over the 105–140 m depth range as from the base of the euphotic zone (nominally 120 m). ^{234}Th and mass fluxes were obtained from sediment traps of the Particle Interceptor Trap (PIT) design, while organic carbon and mass fluxes (along with chlorophyll and other parameters, Rodier and Le Borgne, 1997) were obtained from traps of the Lorenzen design (see Methods). At FLUPAC TS-I and predominantly along Zonal Flux, PIT ^{234}Th (Fig. 7A) fluxes

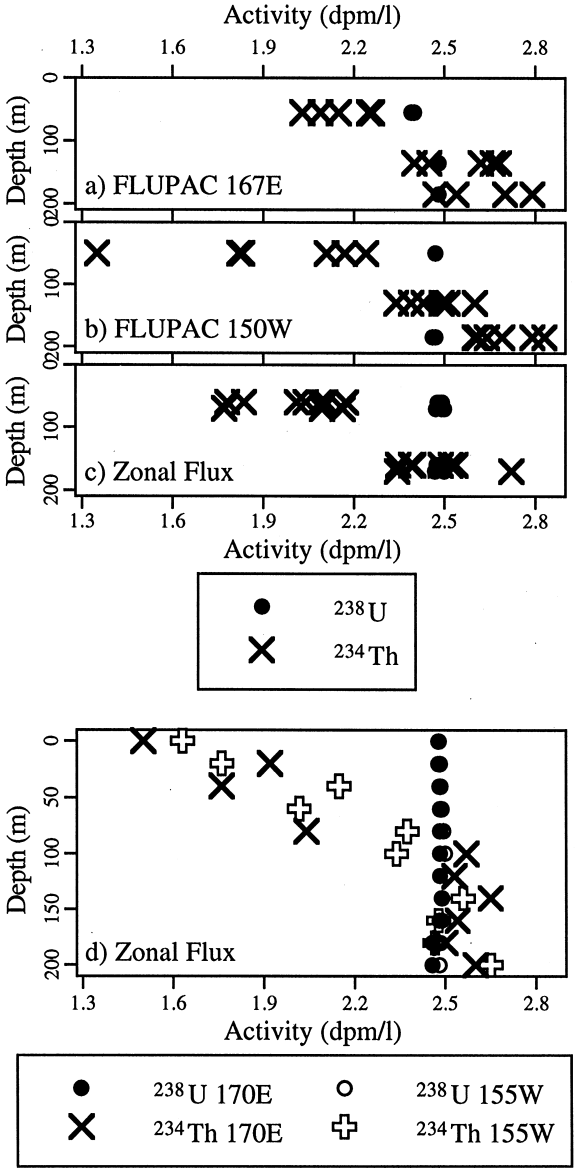

Fig. 6. Average ^{234}Th and ^{238}U activities at the FLUPAC Time Series I site (167°E) using the integrated method in the 0–110 m, 110–160 m and 160–210 m depth intervals (6A), at the FLUPAC Time-Series II site (150°W) in the 0–100 m, 100–160 m and 160–210 m depth intervals (6B) and along the Zonal Flux equatorial transect (165°E–150°W) in the 0–110 m, 110–160 m and 160–210 m depth intervals (6C). ^{234}Th and ^{238}U water column activities (dpm/l) discrete profiles at 170°E and 155°W during the Zonal Flux cruise (6D).

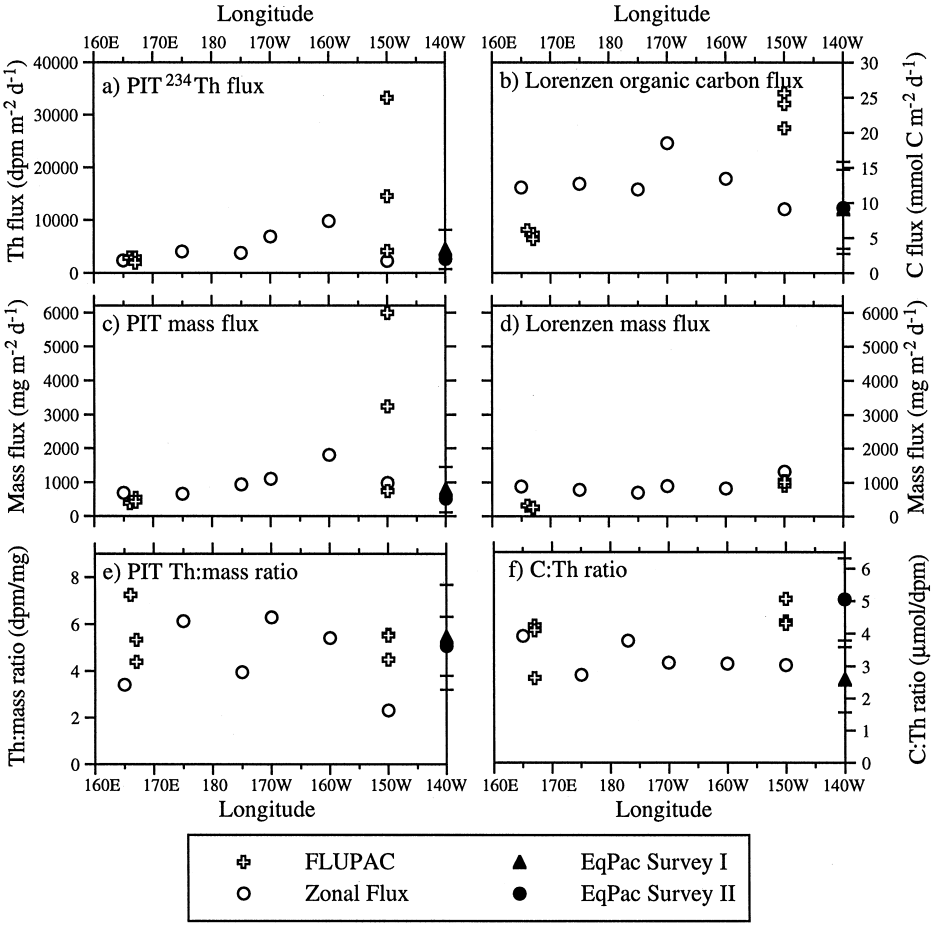

Fig. 7. Sediment trap fluxes at the base of the euphotic zone versus longitude for PIT ^{234}Th (7A; dpm m^{-2} d^{-1}), Lorenzen organic carbon (7B; mmol C m^{-2} d^{-1}), PIT mass (7C; mg m^{-2} d^{-1}), Lorenzen mass (7D; mg m^{-2} d^{-1}), PIT ^{234}Th : mass ratio (7E; dpm/mg) and the PIT ^{234}Th/Lorenzen organic carbon ratio (7F; µmol C/dpm) from the FLUPAC (open crosses) and Zonal Flux (open circles) cruises. Also shown are averages with standard deviations from EqPac at all depths (75–250 m) between 1°N and 1°S for Survey I (filled triangles) and EqPac Survey II (filled circles). The ratio of PIT ^{234}Th : Lorenzen organic carbon is not corrected through mass for the EqPac cruises.

agreed well with observations during EqPac. Relatively high and variable PIT ^{234}Th (Fig. 7A) fluxes were observed at FLUPAC TS-II and slightly elevated fluxes at 160°W during Zonal Flux. Lorenzen trap organic carbon fluxes (Fig. 7B) were much less variable, with low values at FLUPAC TS-I, high values at FLUPAC TS-II and intermediate values during Zonal Flux. PIT mass (Fig. 7C) tracked PIT ^{234}Th fluxes extremely well, leading to a relatively small range in the ratio of ^{234}Th to mass in

sinking material (5.0 ± 1.4 dpm/mg, Fig. 7E), consistent with observations during EqPac (Murray et al., 1996). Lorenzen trap mass fluxes were low at FLUPAC TS-I and intermediate at FLUPAC TS-II and during Zonal Flux. Comparisons of the PIT and Lorenzen trap designs showed only moderate intertrap variability during FLUPAC TS-I and Zonal Flux, but high intertrap variability during FLUPAC TS-II. On the same array, average variability in trap mass flux within the same design was low (17%), while variability in trap mass flux between designs averaged twice that value during FLUPAC TS-I (31%) and Zonal Flux (38%). During FLUPAC TS-II, variability between trap designs was extremely high (195%).

Because of the high occasional variability observed in PITs, which was not observed in the Lorenzen traps, and the tight correlation observed between ^{234}Th and mass in PITs ($r^2 = 0.80$, $n = 50$, $P < 0.001$), mass was used to inter-calibrate between ^{234}Th and organic carbon to obtain the C : ^{234}Th ratio in sinking particles: $(C/^{234}Th) = (C/mass)_{Lor}.\ (mass/^{234}Th)_{PIT}$ (Fig. 7F). Estimated C : ^{234}Th ratios of sinking material at the base of the euphotic zone had no zonal gradient during Zonal Flux. Differences in the C : ^{234}Th ratio between FLUPAC TS-I (3.7 ± 0.9 μmol/dpm) and the entire Zonal Flux transect (3.1 ± 0.5 μmol/dpm) were insignificant ($P > 0.1$), while the FLUPAC TS-II estimates (4.6 ± 0.4 μmol/dpm) were significantly higher at the $P = 0.005$ level (Mann-Whitney U test; Sokal and Rohlf, 1995).

3.1.3. ^{234}Th-based estimates of trap accuracy and POC export

^{234}Th deficiency fluxes and upwelling-corrected deficiency fluxes are shown in Fig. 8. While water column ^{234}Th data was taken based on intended trap depths (Appendix A), actual trap depths based on the trap array pressure sensor varied between 105 and 140 m (Appendix B). We assume that all results apply to the base of the euphotic zone (120 m). This assumption is substantiated by results from the EqPac Survey cruises (Murray et al., 1996), in which sediment trap C : ^{234}Th ratios had intra-station standard deviations averaging only 26% of the mean in the 100 m to 150 m range ($n = 58$). Variability in the ^{234}Th deficiency flux (Fig. 8A) was low ($\pm 40\%$), with the lowest values in the warm pool during FLUPAC TS-I and the highest value at 160°W during Zonal Flux. Values were very similar to those obtained during both EqPac Survey cruises (Fig. 8A). The vertical advection component of the ^{234}Th model increased the total estimated downward flux of ^{234}Th considerably (Fig. 8B). The deficiency flux estimates during Zonal Flux were raised on average by 107% due to the upwelling correction. This is slightly less than the corrections of 121% during EqPac Survey I and 145% in EqPac Survey II (Murray et al., 1996). FLUPAC TS-II fluxes were raised to a lesser degree (70%) while fluxes during FLUPAC TS-I were raised the least (33%). Overall, the flux estimates during FLUPAC were 50% lower at TS-I than at TS-II. Deficiency fluxes during Zonal Flux averaged 34% higher than FLUPAC TS-II and, like the ^{234}Th deficiency fluxes, had no zonal gradient.

Comparison of measured and modeled ^{234}Th fluxes in sediment traps gives an estimate of the degree of trap over-collection for ^{234}Th. Over-collection factors for PITs ($= {}^{234}Th_{PIT}/{}^{234}Th_{model}$) at the base of the euphotic zone (100–140 m) are shown in Fig. 8C. At FLUPAC TS-I, PITs over-collected ^{234}Th by 2.1–2.7 times. At FLUPAC TS-II, PIT over-collection was much higher and more variable, with

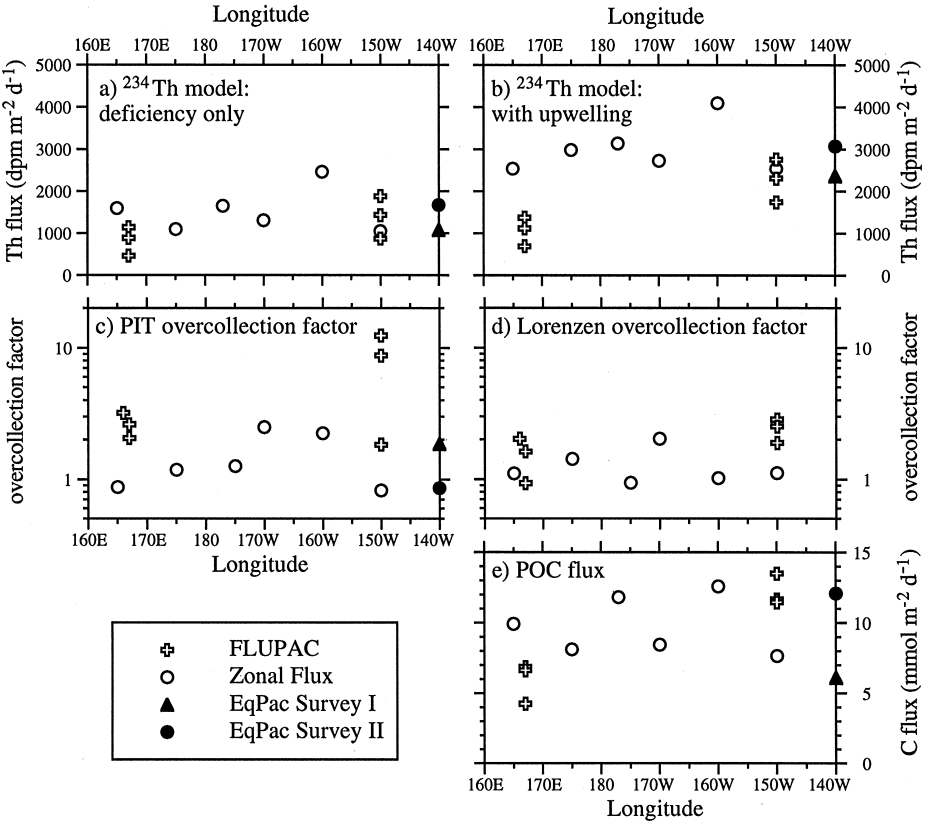

Fig. 8. Model fluxes at the base of the euphotic zone versus longitude for the observed ^{234}Th deficiency (8A; dpm m^{-2} d^{-1}), ^{234}Th deficiency with upwelling correction (8B; dpm m^{-2} d^{-1}), model estimate of PIT overcollection (8C; PIT flux/model flux), model estimate of Lorenzen overcollection (8D; Lorenzen trap flux/model flux), and model particulate organic carbon flux (POC export; 8E; mmol C m^{-2} d^{-1}) from the FLUPAC (open crosses) and Zonal Flux (open circles) cruises. Also shown are data from EqPac Survey I (1°N–1°S; filled triangles) and EqPac Survey II (1°N–1°S; filled circles).

^{234}Th over-collection of 1.8–12.0 times. During the Zonal Flux transect, ^{234}Th over-collection was smaller at 0.9–2.7 times. Over-collection by Lorenzen traps at the base of the euphotic zone (100–140 m) was also estimated: $(^{234}Th_{Lor}/^{234}Th_{model}) = (Mass_{Lor}/Mass_{PIT})$. $(^{234}Th_{PIT}/^{234}Th_{model})$ (Fig. 8D). Lorenzen trap over-collection was moderate, 1.0–2.7. On average, flux correction using ^{234}Th decreased the Lorenzen trap flux by $32 \pm 24\%$ at the base of the euphotic zone.

^{234}Th-based particulate organic carbon fluxes at the base of the euphotic zone (POC export) were relatively invariant in the upwelling region as shown in Fig. 8E. FLUPAC TS-I had the lowest fluxes (5.9 ± 1.4 mmol C m^{-2} d^{-1}), though only slightly lower than EqPac Survey I (6.1 mmol C m^{-2} d^{-1}, 1°N–1°S). Both cruises took place during El Niño conditions. Fluxes at FLUPAC TS-II were

12.2 ± 1.1 mmol C m^{-2} d^{-1}, not statistically different from those during Zonal Flux (9.8 ± 2.1 mmol C m^{-2} d^{-1}; $P > 0.1$). The Zonal Flux POC export estimates demonstrated no significant zonal gradient ($P > 0.1$). These estimates compare well with estimates from EqPac Survey II (12.1 mmol C m^{-2} d^{-1}, 1°N–1°S).

3.1.4. Uncertainty in the ^{234}Th model sinking flux

Uncertainty in ^{234}Th-based particle export fluxes comes from the uncertainty in four components of the ^{234}Th model: the ^{234}Th deficiency relative to ^{238}U, the C : ^{234}Th ratio in sinking particles, effects of circulation on the ^{234}Th deficiency and nonsteady-state effects. Least squares propagated uncertainty in individual measurements of the observed ^{234}Th deficiency averaged $55 \pm 24\%$ for both cruises. Since the FLUPAC cruise utilized two measurements of the ^{234}Th deficiency for each POC export estimate, the overall FLUPAC uncertainty in the deficiency was only 39%. The total observed variability in estimates from both cruises was 43% of the mean. Uncertainty in the C : ^{234}Th ratio in sediment traps at the base of the euphotic zone can also be estimated from the total variability in the data. Without normalization for mass, the C : ^{234}Th ratio for both cruises was 2.8 ± 1.5 μmol/dpm giving a variability of 54%. Normalizing for mass increased the mean by 32% to 3.7 ± 0.8 μmol/dpm and reduced the variability considerably, to 21%.

Uncertainty in the upwelling flux of ^{234}Th was found to have a large impact on flux estimates from EqPac (Buesseler et al., 1995; Murray et al., 1996; Bacon et al., 1996). Least squares propagated uncertainty in the upwelling flux averaged $116 \pm 4\%$ during Zonal Flux assuming an uncertainty in w of 50% and the uncertainty in observed ^{234}Th gradients. This led to an overall uncertainty in the model ^{234}Th flux averaging $67 \pm 12\%$. Because an average of two discrete ^{234}Th profiles obtained during the Zonal Flux was used to estimate vertical ^{234}Th gradients for the FLUPAC cruise, the uncertainty in the upwelling fluxes for FLUPAC is higher than for Zonal Flux. To get a quantitative estimate of this uncertainty, we calculated upwelling fluxes using three hypothetical scenarios. A scenario of linear increase in ^{234}Th from the surface to 120 m gave upwelling fluxes that were $9 \pm 8\%$ lower than the fluxes estimated from the observations. A scenario of linear increase in ^{234}Th from the surface to 60 m (similar to the observations; Fig. 6C) gave upwelling fluxes that were $8 \pm 16\%$ higher than the estimated fluxes from the observations. A scenario of linear increase in ^{234}Th from 60 m to 120 m (the opposite of what was observed) gave upwelling fluxes that were $56 \pm 5\%$ lower than the estimated fluxes from the observations. Overall, the uncertainty in the gradient in ^{234}Th contributed less to the overall uncertainty in the upwelling flux than did the uncertainty in w. Because the FLUPAC cruise took place during an extended period of diminished upwelling, the upwelling fluxes were lower (Fig. 8B). Thus, the overall impact of the uncertainty in upwelling was smaller during the FLUPAC cruise.

Though upwelling is arguably the largest transport term in the ^{234}Th mass balance at the equator (Dunne et al., 1999a), the uncertainty in the other circulation terms also needs to be addressed. Buesseler et al. (1995) showed that zonal advection was a negligibly small flux in the central equatorial Pacific during the EqPac study. This result was confirmed here, as no gradients in ^{234}Th could be observed along the Zonal

Flux transect. Though a difference in ^{234}Th was observed between FLUPAC TS-I and TS-II, these sites were from water masses with very different densities that probably do not mix. Buesseler et al. (1995) and Murray et al. (1996) showed that meridional advection was also a small flux at the equator during the EqPac study. The role of turbulent mixing is less well constrained. Dunne et al. (1999a) suggested that ^{234}Th-based particle export estimates at the equator from EqPac Survey II overestimated the particle export by 33% by neglecting horizontal mixing. Because we have no discrete profiles of ^{234}Th off the equator in this study, we cannot directly evaluate this potential source of variability. Dunne et al. (1999a) suggested, however, that horizontal mixing should be important only during periods of high upwelling. Upwelling velocities in the model were as high as 3.9 m d^{-1} at 40 m and 1.0 m d^{-1} at 120 m. Comparison in terms of relative upwelling suggests that estimates from FLUPAC were the least biased by horizontal mixing, since upwelling velocities estimated for that time period were low (2.1 m d^{-1} at 45 m and -0.6 m d^{-1} at 120 m). Upwelling velocities estimated for the Zonal Flux cruise (3.0 m d^{-1} at 45 m and 0.7 m d^{-1} at 120 m), however, were only slightly less than those estimated for EqPac Survey II (3.9 m d^{-1} at 50 m and 1.1 m d^{-1} at 120 m; Chai, 1995). While ^{234}Th-based FLUPAC estimates of the POC export may be unaffected by horizontal mixing, Zonal Flux estimates may be about 20% too high.

There are two nonsteady-state effects to consider as well: (1) a potential mismatch between the two-day trap deployment and the timescale of ^{234}Th decay ($t_{1/2} = 24$ days) and (2) a time-varying ^{234}Th balance. Short-term variability in particle flux is always possible, specifically with respect to the diurnal cycle. The ^{234}Th method necessarily increases the timescale of the particle export estimate from 2-days to a month. Temporal gradients in the ^{234}Th budget can be assessed from the FLUPAC time-series data, but not from the Zonal Flux data. On the whole, FLUPAC time-series I and II demonstrated little variability in ^{234}Th activities (4.7% during TS-I, 9.6% during TS-II) beyond analytical uncertainty (average 3.4%), consistent with steady state. However, the uncertainty in steady state from the six-day time series alone is extreme. Though the temporal regressions are statistically insignificant ($P > 0.1$), the slope is not well constrained. Because the sampling period for each time series was short relative to the half life of ^{234}Th, the uncertainty in the slope is large and estimates of the temporal term in the ^{234}Th budget of 735 ± 4073 dpm m^{-2} d^{-1} for the upper 110 m during TS-I and -1319 ± 5376 dpm m^{-2} d^{-1} for the upper 100 m during TS-II. Because the slopes were insignificant and presumably due to analytical uncertainty rather than natural variability, however, we ignore the temporal component of the ^{234}Th balance in this study.

4. Discussion

4.1. Variability in trap collection efficiency

Though sediment trap collection efficiency has been widely studied (Butman et al., 1986a,b; Baker et al., 1988; Gardner et al., 1997), it remains a field of some mystery.

Table 1
^{234}Th : mass ratios (mg/dpm) for swimmers and net tow material collected at the equator, 150°W, during the FLUPAC cruise

Sample type	Length (mm)	^{234}Th/mass (dpm/mg)
Phytoplankton aggregates	> 2	1.67 ± 0.21
Foraminifera	1–2	1.16
200–500 μm net tow	0.2–0.5	0.55 ± 0.02
500–2000 μm net tow	0.5–2.0	0.53 ± 0.05
Copepods	2–3	0.31 ± 0.01
Euphausiids	6–9	0.084 ± 0.003
Chaetognaths	13–17	Low (< 0.02)
Caridae	25	Low (< 0.02)
Gelatinous material	> 10	Low (< 0.02)

Butman et al. (1986a) conducted experiments suggesting that velocity (discussed as the Reynolds number) tends to induce under-trapping in baffled, cylindrical traps but induced over-trapping in other trap geometries. Similarly, Baker et al. (1988) found that traps allowed to drift with the current caught more material than moored traps at current velocities above 12 cm s^{-1}. This suggests either that moored traps under-collect material or that drifting traps over-collect. Butman et al. (1988b) synthesized data with simple theories of sediment transport. They explained under-trapping in cylindrical traps through shear-induced resuspension of particles either at the trap mouth or the brine interface. They also suggested three explanations for over-trapping: (1) the effective diameter is larger than the diameter at the mouth. This is not a concern for cylindrical traps. (2) Adsorption of particles onto the walls of the container would decrease the concentration of particles. Mixing with overlying water would replace particles leading to a net diffusive flux into the trap. (3) Increased turbulence (shear) at the trap mouth can enhance coagulation. Both 2 and 3 are possibilities.

Inter-trap variability in the flux of material caught in sediment traps of the PIT design at FLUPAC TS-II is also a matter of some concern. Swimmers, hydrodynamic biases and temporal variability in flux are all potential sources of variability. ^{234}Th : mass ratios measured for a variety of potential swimmer contaminants are shown in Table 1. These swimmers all have ^{234}Th : mass values much lower than the values obtained in traps. Because the ^{234}Th : mass ratio in sediment traps was invariant (Fig. 7E), we reject the possibility of swimmer contamination. Because traps of the Lorenzen design did not collect highly variable amounts of material, we reject the possibility of natural temporal variability in the sinking flux. This leaves hydrodynamic bias as the most probable source of PIT variability. Using the R/V *l'Atalante*'s acoustic Doppler current profiler (ADCP) and the trajectory of the sediment traps, we estimated the average velocity of water across the top of the traps during FLUPAC. Most of the velocity across the traps was due to zonal shear between the surface and the eastward propagating equatorial undercurrent at the depth of the traps. At FLUPAC

TS-I, average velocities of sediment traps relative to the flow were estimated to have been in a fairly small range between 17 and 21 cm s^{-1} relative to the average water velocity of 25 cm s^{-1}. At FLUPAC TS-II, average velocities of sediment traps relative to the flow were twice those at TS-I, also in a fairly small range between 36 and 41 cm s^{-1} relative to the average water velocity of 62 cm s^{-1}. Given the results of Baker et al. (1988), these results suggest that the higher horizontal shear across the water-trap interface at FLUPAC TS-II increased the amount of material caught in PITs. We necessarily assume in this study that the processes effecting the collection efficiency of the traps did not fractionate the sinking particle pool with respect to carbon, mass and ^{234}Th.

The same types of sediment traps used to collect ^{234}Th and organic carbon in this study were used in the EqPac program (Murray et al., 1996). As no inter-calibration using mass was possible during EqPac, it is important to ascertain whether the EqPac traps suffered inter-trap collection biases as observed at FLUPAC TS-II, which would alter the estimated C : ^{234}Th ratio. If traps of the PIT design measured for ^{234}Th had indeed collected more material than those of the Lorenzen design measuring C, then C : ^{234}Th values would have been artificially low. Fortunately, EqPac C : ^{234}Th ratio estimates did not have spurious low values, leading us to conclude that this differential hydrodynamic bias between traps observed at FLUPAC TS-II was not an important factor during EqPac.

4.2. *C* : ^{234}Th *ratios of sinking particles*

Sediment traps are currently the only means of directly collecting sinking particles. Results from sediment trap studies have often been disputed, however, under the premise that swimmer contamination biases the data towards higher C : Th ratios relative to representative sinking particles. In situ filtration has often been used to collect particles and generally results in lower C : ^{234}Th ratios (0.5–2.5 μmol/dpm; Buesseler et al., 1995; Bacon et al., 1996; Murray et al., 1996; Charette et al., 1999). C : ^{234}Th ratios based on drifting sediment trap samples near the base of the euphotic zone from various studies are shown in Table 2. Comparison of these studies shows remarkable consistency suggestive of two things:

(1) The C : ^{234}Th ratio of sinking particles in these studies has a relatively narrow range. Adsorption rate constant estimates (Bacon and Anderson, 1982; Coale and Bruland, 1985; Dunne et al., 1997) suggest that the C : Th ratio should decrease over the timescale of a month to a point at which particles come to a steady-state of adsorption, desorption, decay and sinking. Thus, we would expect to see large differences in C : Th ratios of sinking particles between steady-state production and the termination of phytoplankton blooms, between sinking aggregates and fecal pellets, and between oceanic regimes dominated by differential size classes of phytoplankton and zooplankton. We speculate that the narrow range of C :Th ratios in these particles is due to the fact that either the particles had come into equilibrium with respect to ^{234}Th sorption or the process of particle reprocessing and sinking had

Table 2
C : ^{234}Th ratios (μmol/dpm) and their variability (1 s.d.) from drifting sediment traps near the base of the euphotic zone from various studies

Study	C : ^{234}Th ratio (μmol/dpm)	Reference
FLUPAC TS-I	3.7 ± 0.9	This study
FLUPAC TS-II	4.6 ± 0.4	This study
Zonal Flux	3.1 ± 0.5	This study
EqPac Survey I	2.8 ± 1.1	Murray et al. (1996)
EqPac Survey II	3.6 ± 1.8	Murray et al. (1996)
North Atlantic Bloom Experiment	4.5 ± 1.8	Buesseler et al. (1992)
Bermuda Atlantic Time-series	7.0 ± 0.5	Buesseler et al. (1994)
Subarctic northeast Pacific	3.3 ± 1.8	Charette et al. (1999)
Santa Barbara Channel	3.5 ± 0.8	Dunne (1999)
Hawaii Ocean Time-series	5.6	Dunne (1999) and J. Murray (unpublished)

a similar timescale at these sites such that the sinking particles were at similar degrees of ^{234}Th adsorptive disequilibrium.

(2) Sediment traps can be reproducibly picked of swimmers. Because swimmers have essentially no ^{234}Th, their presence in the samples skews the data so that the frequency distribution has a long tail at high C : Th ratios. In their analysis of the EqPac data, Murray et al. (1995) found significant skew to the data. They performed log transformations to eliminate this skew overall and used Chauvenet's criterion for rejecting spuriously high C : Th ratio data on a station by station basis. During FLUPAC and Zonal Flux, frequency distributions of the data were not skewed, possibly because of our improved method of picking swimmers (first by naked eye, then by microscope, then by naked eye).

4.3. Comparison of conditions in October 1994 and April–May 1996

One goal of this study was to establish variability in POC export both zonally between the western and central equatorial Pacific and temporally between season and El Niño-Southern Oscillation (ENSO) condition. Results are summarized in Table 3. Relatively low POC export was observed in the warm pool at TS-I (5.9 ± 1.4 mmol C m^{-2} d^{-1}), consistent with the observation that the region was devoid of nitrate in the upper 2/3 of the euphotic zone (Fig. 4). TS-I also exhibited low inventories of particulate organic carbon and chlorophyll and low levels of integrated primary production (Table 3). High levels of POC export were observed at FLUPAC TS-II (12.2 ± 1.1 mmol C m^{-2} d^{-1}), consistent with the euphotic zone having 3–9 μM nitrate (Fig. 4), higher inventories of particulate organic carbon and chlorophyll and extremely high integrated primary production (Table 3). POC export (9.8 ± 2.1 mmol C m^{-2} d^{-1}), nitrate concentrations and chlorophyll inventories along the Zonal Flux transect were similar to values observed at FLUPAC TS-II. Integrated primary production was lower along Zonal Flux than at FLUPAC TS-II,

Table 3
Summary of sea surface temperature (SST; °C) and nitrate ($SSNO_3$; μM), water column inventories (0–120 m) of total particulate carbon (∫PC; mmol C m^{-2}) and chlorophyll (∫Chl; mg Chl m^{-2}), integrated ^{14}C primary production (∫PP; mmol C m^{-2} d^{-1}; A. LeBoutelier, Z. Johnson, personal communication) and $^{15}NO_3$ new production * 6.6 (∫NP; mmol N * 6.6 m^{-2} d^{-1}; A. LeBoutelier, A. Aufdenkampe et al., submitted) and POC export (mmol C m^{-2} d^{-1}) during FLUPAC and Zonal Flux. EqPac data for SST, $SSNO_3$ and ∫PC were taken from the JGOFS data base, ∫Chl and ∫PP from Barber et al. (1996). ∫NP was taken from McCarthy et al. (1996) for the EqPac Surveys and from Bacon et al. (1996) for the Time-series. POC export was taken from Murray et al. (1996) for the EqPac Surveys. For the EqPac Time-series, POC export was estimated using ^{234}Th particulate fluxes from Bacon et al. (1996) and data on the C : ^{234}Th ratios in sediment traps from the EqPac Surveys between 1°N and 1°S (Murray et al., 1996) with the original estimate given in parentheses

Station	Dates	SST	$SSNO_3$	∫PC	∫Chl	∫PP	∫NP	POC export
FLUPAC-0°N								
TS I, 165°E	Oct. 1994	29.3 ± 0.3	0.00 ± 0.00	313 ± 69	19 ± 3	60 ± 5	9.9 ± 1.0	5.9 ± 1.7
TS II, 150°W	Oct. 1994	27.2 ± 0.1	2.85 ± 1.89	401 ± 72	25 ± 3	126 ± 4	13.9 ± 0.8	12.2 ± 3.5
Zonal Flux-0°N								
165°E	Apr. 1994	28.2 ± 0.2	3.03 ± 0.07	561 ± 52	34 ± 3	71 ± 21	6.4	9.9 ± 7.0
175°E	Apr. 1994	27.8 ± 0.1	2.94 ± 0.08	493 ± 36	25 ± 4	87 ± 8	19.2	8.1 ± 6.9
177°W	Apr. 1994	27.4 ± 0.2	4.32 ± 0.05	600 ± 98	27 ± 6	80 ± 41	16.0	11.8 ± 9.8
170°W	May 1994	27.3 ± 0.1	4.15 ± 0.08	555 ± 47	26 ± 4	89 ± 11	17.0	8.4 ± 6.3
160°W	May 1994	27.0 ± 0.0	4.72 ± 0.06	455 ± 29	27 ± 7	82 ± 9	21.1	12.6 ± 6.3
150°W	May 1994	26.3 ± 0.1	5.49	478	21 ± 2	75 ± 2	29.2	7.7 ± 6.6
EqPac-140°W								
Survey I, 1°N-1°S	Feb. 1992	28.5 ± 0.1	2.83 ± 0.17	240 ± 46	25 ± 1	60 ± 8	3.8 ± 0.9	5.3 ± 1.6
Time-series I, 0°N	Mar.–Apr. 1992	28.5 ± 0.2	2.83 ± 0.25	468 ± 82	29 ± 1	90 ± 3	15 ± 7	6.7 (1.9)
Survey II, 1°N-1°S	Aug. 1992	25.1 ± 0.5	5.97 ± 0.38	320 ± 93	32 ± 2	101 ± 8	17.1 ± 7.2	12.1 ± 3.0
Time-series II, 0°N	Oct. 1992	25.1 ± 0.3	5.76 ± 1.21	529 ± 79	33 ± 2	129 ± 6	22 ± 10	12.8 (2.4)

while particulate organic carbon inventories were slightly higher. In general, the effect of El Niño was to change the geographic extent of the equatorial upwelling zone as defined by super-μM nitrate and, subsequently, the geographic extent of high POC export. Beyond this, however, no influence of El Niño on primary production, new production or POC export was observed during FLUPAC.

4.4. POC export during EqPac

During the EqPac survey cruises, five different methods were used to estimate particle export: cylindrical sediment traps (PIT and Lorenzen; Murray et al., 1996), conical sediment traps (Internal rotating sphere or IRS; Hernes et al., 1996), ^{234}Th disequilibria combined with sediment trap C : Th (Murray et al., 1996), ^{234}Th disequilibria combined with in situ filtered C : Th (Murray et al., 1996), and ^{230}Th and ^{228}Th disequilibria combined with in situ filtration (Luo et al., 1995). Particle export was also estimated from ^{234}Th disequilibria combined with in situ filtered C : Th during the EqPac Time-series cruises (Bacon et al., 1996) and during the NOAA survey cruises (Buesseler et al., 1995). These various methods resulted in highly divergent values of POC export for 1992 boreal fall. Quay (1997) compiled all available estimates of carbon fluxes from EqPac to statistically evaluate the equatorial carbon mass balance. He showed that three of the five POC export estimates for boreal fall, 1992 [(1) conical sediment traps, (2) ^{234}Th disequilibria combined with in situ filtered C : Th, and (3) ^{230}Th and ^{228}Th disequilibria combined with in situ filtration] implied a large, unexplained carbon imbalance for this time period. We suggest that these three methods gave artificially low values for the following reasons:

(1) Conical sediment traps have been previously shown to strongly under-collect sinking material in high shear environments (Butman et al., 1986). Low POC export estimates from conical sediment traps might be expected in the vigorous current regime of the equatorial Pacific. Hernes et al. (submitted) showed that even though the conical traps undercollected ^{234}Th flux by large and variable amounts, the C : Th ratios in PIT (3.6 ± 1.8 μmol/dpm) and IRS traps (5.0 ± 0.7 μmol/dpm; excluding those deployments with ^{234}Th-derived collection efficiencies below 10%) during the EqPac Survey cruises were similar. Because of this, the ^{234}Th-based POC fluxes based on conical traps are also similar to those from PITs (Hernes et al., submitted).

(2) During EqPac, the method of combining ^{234}Th disequilibria with in situ filtered C : Th was also tested as a means of estimating POC export (Buesseler et al., 1995; Bacon et al., 1996). One of the primary assumptions of this method is that the C : Th ratio in suspended particles equals that in sinking particles. This assumption has not been directly tested and is based on models of simple particle and ^{234}Th cycling (e.g. Bacon and Anderson, 1982). As $> 90\%$ of particles in this region remineralize rather than sink, there is a large potential for differential particle cycling as discussed in Dunne et al. (1997). One particle-^{234}Th cycling model, which considers two particle types, distinguishes between suspended, refractory particles in equilibrium with ^{234}Th (low C : Th ratios) and sinking, labile particles in adsorptive disequilibrium (high C : Th ratios). Alternatively, the large size of sinking particles may provide a small

effective surface area to volume ratio, adsorbing relatively low levels of ^{234}Th (high C : Th ratios) at equilibrium. There are many possible mechanistic scenarios that may be at work. Because of the relative ease of estimating POC export using in situ filtration compared to sediment traps, this method is extremely attractive and deserves a great deal of future research including field and model validation.

(3) In addition to the issue of in situ filtration driving low C : Th ratios, we suggest that POC export estimates based on ^{230}Th and ^{228}Th disequilibria combined with in situ filtration (Luo et al., 1995) are low because of a mismatch in time scales. The residence time of water in the equatorial region is short (months) while that of upwelled water near the equator is very short (weeks). This vigorous circulation had a large impact on ^{234}Th results from EqPac (Buesseler et al., 1995; Murray et al., 1996; Bacon et al., 1996; Dunne and Murray, 1999), even with its relatively short half life of 24 days. The half-life of ^{228}Th is 1.9 years while the half-life of ^{230}Th is 75,000 years. As a consequence, these isotopes integrate a much longer/larger scavenging history/region. ^{230}Th and ^{228}Th are nearly fully scavenged in the upper 100 m and do not come into equilibrium until well below the euphotic zone (Luo et al., 1995), making them insensitive to variability in POC export at 120 m. Neither advection nor nonsteady state terms were considered in the Luo et al. (1995) analysis, which focused on the deeper biogeochemical scales to which these isotopes are much better suited.

The Quay (1997) synthesis calls into serious question these means of estimating particle export. Thus, in the following sections we compare our results only with POC export estimates from ^{234}Th disequilibria combined with sediment trap C : Th. In order to utilize data from the EqPac Time-series cruises, we have recalculated the ^{234}Th based Bacon et al. (1996) POC export estimates for the EqPac time-series cruises using sediment trap C : ^{234}Th ratios from the respective EqPac Survey cruises (Table 3).

4.5. Comparison with results from the EqPac surveys

Comparison with EqPac allows us to more fully explore the role of the large scale physical forcing (seasonal cycle and ENSO condition) on POC export in the western and central equatorial Pacific. Whereas the EqPac program studied boreal spring, El Niño conditions and boreal fall, non-El Niño conditions, the Zonal Flux cruise took place during boreal spring La Niña conditions and the FLUPAC cruise during boreal fall conditions of El Niño. POC export was low during EqPac Survey I and FLUPAC TS-I and high during EqPac Survey II, FLUPAC TS-II and the entire Zonal Flux transect. The observation of low POC export at FLUPAC TS-I (5.9 ± 1.4 mmol C m^{-2} d^{-1}) is consistent with nitrate limitation of the food web in the upper half of the euphotic zone due to the presence of the warm pool (Figs. 3 and 4). POC export values were similar during EqPac Survey I and Survey II (Murray et al., 1996) at stations with the euphotic zone dominated by sub-μM nitrate (4.1 ± 2.1 mmol C m^{-2} d^{-1}; 12°N, 9°N, 7°N, 5°N, 12°S). At all other sites nitrate levels were super-μM throughout the euphotic zone and demonstrated higher POC export, averaging 8.5 ± 4.5 mmol C m^{-2} d^{-1} for all 4 cruises.

Given the relatively invariant POC export observed near the equator (1°N–1°S) during Survey II, FLUPAC TS-II and Zonal Flux, we are left to explain only the low POC export observed in the HNLC region during EqPac Survey I (3.5 ± 1.7 mmol C m^{-2} d^{-1}; 3°N–5°S) and the extremely high export during EqPac Survey II at 2°N (19.5 mmol C m^{-2} d^{-1}). Given the high POC export at FLUPAC TS-II (boreal fall, El Niño) and during Zonal Flux (boreal spring, non-El Niño), we conclude that the low POC export observed during the EqPac Survey I cruise (boreal spring, El Niño) can be explained by neither seasonal nor El Niño variability individually. Conversely, the high POC export observed during the EqPac Survey II cruise (boreal fall, non-El Niño) is equally attributable to either seasonal or El Niño variability. Assuming that seasonal and El Nino forced variability are the dominant sources of POC export variability, these combined results suggest that only the combination of seasonal and El Niño effects on equatorial upwelling have an observable effect on POC export within the HNLC region. In addition to seasonal and ENSO conditions, equatorial waves provide a source of upwelling variability that may determine variability in primary production, new production and POC export within the HNLC region.

4.6. The role of equatorial waves

Two forms of equatorially trapped waves provide for a significant portion of equatorial Pacific variability (Philander, 1990; Kessler and McPhaden, 1995) (Fig. 9). The first of these, the equatorial Kelvin Wave, is formed by westerly wind bursts piling up water onto the equator while water on the equator gets pushed eastward and downward. The subsequently elevated sea surface height and corresponding depression in the thermocline is rapidly translated eastward at about 2.0–2.3 d^{-1}, with intense downwelling and subsequent upwelling of the thermocline with a period of 1–2 months determined by the zonal and temporal extent of the wind burst (Fig. 9A). The second type of wave, the Tropical Instability Wave (a.k.a. TIW, long wave, Legeckis wave, 21-day wave, 28-day wave), takes the approximate form of a Rossby Wave as variability in easterly winds pulls water westward and poleward, giving it an anticyclonic tendency. North of the equator, these waves are amplified by the shear between the South Equatorial Current and the North Equatorial Countercurrent horizontal advection, the meridional currents advecting cool equatorial surface water northward and warm NECC water southward while developing intense upwelling near the equator and intense downwelling at the western, leading edge (Fig. 9B). Kelvin waves tend to inhibit upwelling of cold, nutrient-rich water into the euphotic zone, and TIWs tend to enhance it (Flament et al., 1996; Harrison, 1996).

We hypothesize that Kelvin wave and Tropical Instability Wave (TIW) activity, rather than large scale seasonal or ENSO variability, may have caused the observed variability in POC export between the EqPac Survey I, EqPac Survey II, FLUPAC and Zonal Flux cruises. Kessler and McPhaden (1995) showed that the EqPac Survey I and Time-series I cruises took place under the influence of Kelvin waves, while the EqPac Survey II and Time-series II cruises took place during a period of intense TIW activity.

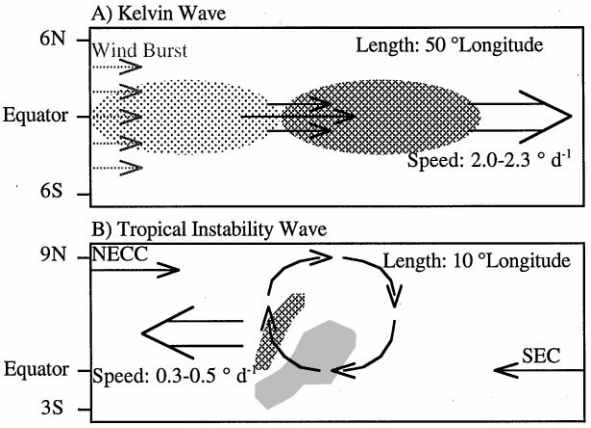

Fig. 9. Schematic of propagation and advection associated with a Kelvin Wave (Philander, 1990; 9A) and a Tropical Instability Wave (Flament et al., 1997; Harrison, 1997; 9B). Propagation (double black arrows), horizontal water motions (single black arrows) and inferred downwelling (hatched areas) and upwelling (gray areas) are shown. Forcing by wind (9A; gray arrows) and the shear between the North Equatorial Counter Current (NECC) and the South Equatorial Current (SEC) are also illustrated.

Interpretation of data from the JGOFS EqPac Time-series II (Foley et al., 1997) and Survey II (Archer et al., 1997b) cruises showed that TIWs can have a potent impact on biogeochemistry of the equatorial Pacific. During the beginning and end of EqPac Time-series II, primary production was $8 \pm 11\%$ higher than during the EqPac Time-series I cruise (Barber et al., 1996). The passage of the TIW was characterized by positive meridional velocity, low temperature and high salinity, nutrients and chlorophyll (Foley et al., 1997). Rates of primary production increased an additional $23 \pm 14\%$ over ambient values during the passage of a TIW. EqPac Survey II encountered a convergent front associated with a TIW at 2°N, with an impressive accumulation of Rhizoselenia at the surface (Yoder et al., 1994; Archer et al., 1997a,b) and increased biological activity all through the water column between 1°N and 2°N (Dunne et al., 1999b). New production and POC export at 2°N associated with the cold water south of the front was estimated at 33 mmol C m^{-2} d^{-1} (McCarthy et al., 1996) and 20 mmol C m^{-2} d^{-1} (Murray et al., 1996), respectively. At the equator, nutrients, particle concentrations and fluxes were similar to those observed during EqPac Time-Series II before and after the passage of the TIW (Table 3). Chavez et al. (1998) showed that Kelvin Waves posed strong forcing on chlorophyll concentrations at a mooring at the equator, 155°W during the onset of the 1997–1998 El Niño.

Though the FLUPAC cruise took place during a strong El Niño, export at FLUPAC TS-II was high relative to EqPac Survey I cruise. Eldin et al. (1997) showed that the FLUPAC cruise track followed the path of a Kelvin wave that preceded the

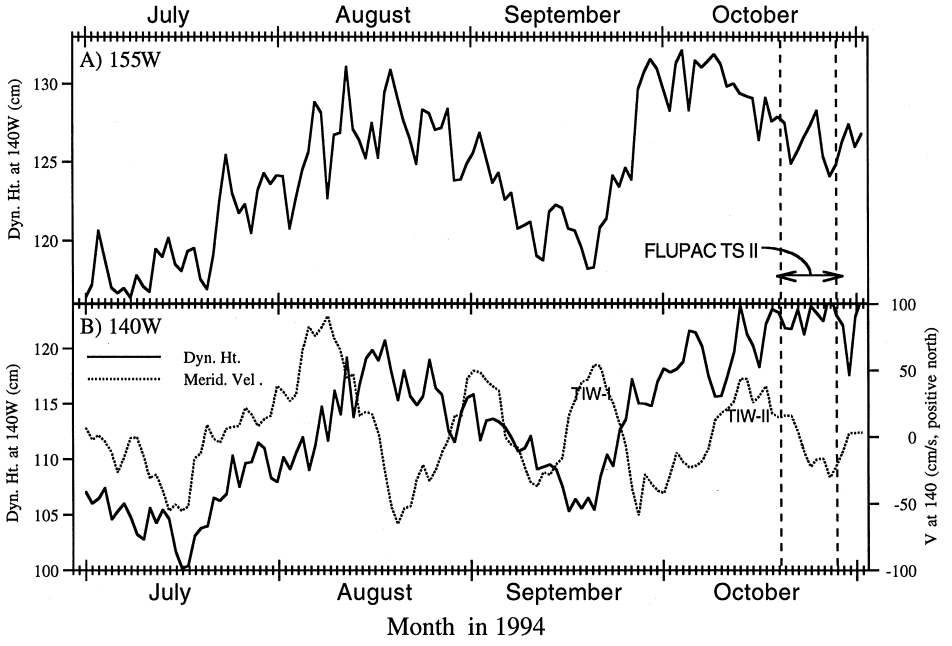

Fig. 10. Data from TOGA-TAO buoys on the equator for July through October, 1994, showing dynamic height (cm) at 155°W (10A) and dynamic height (cm) along with surface meridional velocity (cm/s) at 140°W (10B).

cruise by approximately 20 days. They also noted the presence of TIW activity at the equator, 155°W, using dynamic height data from the TOGA-TAO array. Both Kelvin wave and TIW activity are evident in the TOGA-TAO data on the equator at 155°W (Fig. 10A) and 140°W (Fig. 10B). Two Kelvin waves are clearly seen in the variability of the dynamic height at both stations — one peaking in August and the other in October. Strong TIW activity is apparent in the variability in the meridional velocity at 140°W. Fourier analysis of the data gave a strong peak at a TIW-scale wavelength of 22 days. While Kelvin waves propagate rapidly eastward at approximately 1.8°/day, TIWs propagate westward at only 0.5°/day. Given these timescales of propagation, the strong northward meridional velocity signal during 9/16–9/22 (TIW-I in Fig. 10B) would have passed the FLUPAC TS-II site around 10/9. FLUPAC TS-II took place two weeks later, 10/19–10/28. We suggest that the rise in dynamic height at the end of September (corresponding to an increased heat inventory in the upper ocean) and lowering of dynamic height during October was due to the passage of a Kelvin Wave. The peak in northward meridional velocity at 10/10–10/13 (TIW-II in Fig. 10B) would have reached 150°W at the end of FLUPAC TS-II. Though this TIW would have arrived too late to affect the beginning of TS-II, it is a possible explanation for the observation in the ^{234}Th data of decreased ^{234}Th and nitrate deficit at its end (Fig. 6).

In contrast to FLUPAC, the Zonal Flux cruise took place during a period of neither Kelvin wave (characteristic of the La Niña condition) nor TIW activity (characteristic of the boreal spring). Results from Zonal Flux demonstrate that the presence of TIWs is not a necessary condition for POC export to be as high as it was during EqPac Survey II. However, it appears that TIWs serve to stimulate production both under conditions of diminished upwelling (FLUPAC TS-II relative to EqPac Survey I) and under non-El Niño conditions (EqPac Survey II north of the equator and EqPac Time-Series II relative to Zonal Flux). The observation of slightly lower primary production and particle export estimates during Zonal Flux relative to FLUPAC TS-II suggests that during FLUPAC the TIW-effect of food web stimulation (EqPac Time Survey II) outweighed the Kelvin wave-effect of production suppression (EqPac Survey I).

As Kelvin wave activity is characteristic of El Niño, particularly during its onset (Kessler and McPhaden, 1995), there should be a correlation between the suppression of new, total and export production and El Niño. We suggest that the suppression of production observed during EqPac Survey I as part of the overall El Niño condition was specifically a response to Kelvin wave activity rather than a general feature of the El Niño. The correlation between season and production should prove to be more robust, however, through the strong seasonality of TIWs.

4.7. Modes of POC export variability

In this section, we synthesize the data discussed in the previous sections into three modes of POC export variability: nutrients, large-scale physics and mesoscale physics. These modes are summarized in Table 5. Nutrient forcing is readily apparent in contrasting POC export estimates from EqPac and FLUPAC outside the HNLC region (4.5 ± 2.0 mmol C m^{-2} d^{-1}) and from EqPac, FLUPAC and Zonal Flux data from within the HNLC region (8.7 ± 4.3 mmol C m^{-2} d^{-1}). The presence of nitrate (> 1 μM) appears to double POC export.

To evaluate the potential role of large-scale (ENSO and season) physical forcings in determining variability in POC export, we grouped the data by the presence or absence of El Niño and whether or not the cruise took place in the boreal fall season (Table 5). We found that season alone accounted for 34% of the variability in the data sets while ENSO alone could account for 27% of the variability. We then performed a multiple linear regression to determine that overall, large scale physical forcing could account for 43% of the variability. In the boreal spring, in absence of El Niño, the regression predicted a POC export of 8.3 ± 1.2 mmol C m^{-2} d^{-1}. El Niño accounted for a decrease in POC export by 2.8 ± 1.4 mmol C m^{-2} d^{-1}. Boreal fall accounted for an increase in POC export of 3.8 ± 1.4 mmol m^{-2} d^{-1}. Combined, the net effect of El Niño and boreal fall was a slight increase of 1.8 ± 1.9 mmol C m^{-2} d^{-1}.

We then performed the same analysis by grouping the same data set into the presence of mesoscale (TIW and Kelvin wave) physical forcing (Table 5). We found that the presence of TIWs alone could account for 47% of the variability in the data sets while Kelvin waves alone could account for 18% of the variability. We then

Table 4
Model II slopes, 95% confidence intervals of slopes and squared correlations for the regression of total organic carbon (TOC) versus $6.6 * NO_3$ for EqPac surveys I and II, FLUPAC and Zonal Flux using all data between 2°N and 2°S in the upper 120 m

Cruise	Slope	Range (95% level)	r^2
EqPac Survey I	−0.22	−0.16, −0.28	0.62
EqPac Survey II	−0.24	−0.22, −0.26	0.92
FLUPAC	−0.27	−0.25, −0.29	0.74
Zonal Flux	−0.17	−0.13, −0.20	0.55

Table 5
Summary of large scale (ENSO and season) and mesoscale (TIW and Kelvin wave) physical forcing during the EqPac, FLUPAC and Zonal Flux cruises

Cruise	ENSO	Boreal Season	Equat. Waves
EqPac Survey I	El Niño	Spring	Kelvin
Time-series I	El Niño	Spring	None
Survey II	Normal	Fall	TIW (0°–2°N)
Time-series II	Normal	Fall	TIW
FLUPAC	El Niño	Fall	Kelvin, TIW
Zonal Flux	Normal	Spring	None

performed another multiple linear regression to determine that overall, mesoscale physical forcing could account for 61% of the variability. This is a much higher component of the variability than was accounted for by large scale forcing. In absence of TIWs and Kelvin waves, the regression predicted a POC export of 7.7 ± 0.7 mmol C m^{-2} d^{-1}. The presence of TIWs accounted for an increase in POC export by 5.9 ± 1.1 mmol C m^{-2} d^{-1}. The presence of Kelvin waves accounted for decrease in POC export of 3.4 ± 1.1 mmol m^{-2} d^{-1}. Combined, the net effect of TIWs and Kelvin waves was to increase POC export by 2.5 ± 1.5 mmol C m^{-2} d^{-1}. Though these results are purely descriptive, statistical assessments, they are very suggestive that mesoscale physical forcing dominates POC export variability within the HNLC region.

4.8. Comparison with ^{15}N new production and total organic carbon

^{234}Th-calibrated sediment trap carbon fluxes are not the only estimates of net biological production available for these cruises. Integrated ^{15}N new production from FLUPAC (Rodier and Le Borgne, 1997) and Zonal Flux (Aufdenkampe et al., submitted) were greater than POC export (Table 3). The difference between these two estimates may be due to either a recent temporal increase in new production (the ^{15}N estimate integrates only a day while the ^{234}Th estimate integrates over a month)

or a steady-state accumulation and transport of total organic carbon (TOC). Assuming that ^{15}N new production should vary both above and below the monthly mean, we consider the data set of all four cruises as a whole to minimize the problem of non-steady state. The difference between ^{15}N new production and POC export for the EqPac Survey Cruises (entire transect: 12°N–12°S), FLUPAC and Zonal Flux gives a mean TOC accumulation and transport of 22 ± 46% of new production ($n = 35$).

The role of accumulation and transport of total organic carbon (TOC) was evaluated directly using the regression of TOC against $6.6 * NO_3$ (6.6 = Redfield conversion from nitrogen to carbon) in the upper 120 m for EqPac Surveys I and II, FLUPAC and Zonal Flux (Tables 4 and 5) using Model II analysis (principal axis or major axis regression; Sokal and Rohlf, 1995). This analysis is very similar to that performed previously by Hansell et al. (1997a,b), who found that approximately 20% of new production accumulated as TOC using Model I analysis (least squares regression) of TOC against total inorganic carbon and $6.6 * NO_3$ from NOAA-OACES and FLUPAC data. The range of slopes in our analysis was small, between 0.17 (Zonal Flux) and 0.27 (FLUPAC), implying that 17–27% of new production accumulates as TOC in the equatorial Pacific. This estimate is consistent with previous interpretations: Hansell et al. (1997b) using property–property regressions; Quay et al. (1997) using a mass-balance approach; Archer et al. (1997a) using an inverse model of TOC incorporated into the 3-D flow field from a high-resolution equatorial Pacific general circulation model to estimate the grow-in timescale of TOC upon contact with the euphotic zone.

4.9. Export along the equator in the Pacific

This study answered a number of important questions remaining after the JGOFS EqPac study and re-evaluated variability in equatorial Pacific export production as the expression of three features: surface nitrate, Kelvin waves (or the combination of seasonally low upwelling and El Nino low upwelling) and TIWs. The first-order forcing function of equatorial export is the presence or absence of nitrate. Compared to POC export in the oligotrophic north Pacific at the Hawaii Ocean Time-series (HOT; 2 mmol C m^{-2} d^{-1}; Michaels et al., 1994; Karl et al., 1995), results from EqPac Survey I and Survey II (4 mmol C m^{-2} d^{-1}; 12°N, 9°N, 7°N, 5°N, 12°S; Murray et al., 1996) showed that the presence of subsurface nitrate roughly doubled POC export. Within the HNLC region, POC export doubled once again to between 8 and 12 mmol m^{-2} d^{-1}. While export of dissolved organic carbon at HOT has been shown to account for a large portion (~50%) of total export (Emerson et al., 1997), TOC accumulation and transport accounts for only about 22% of total export in the equatorial Pacific HNLC region.

As has been a general observation in the equatorial Pacific HNLC region beginning with the work of Barber and Chavez (1991), biomass and production appear insensitive to nutrient concentration at the equator. This study found no direct evidence of export dependency on nutrient concentration beyond the condition of no surface nutrients resulting in low export during FLUPAC TS-II). EqPac observations of low export during Survey I (El Niño, boreal spring) and high export during Survey II

(non-El Niño, boreal fall) were previously attributed to an unknown combination of seasonal and El Niño effects. Given the high export at the nitrate rich site of FLUPAC (El Niño, boreal fall) and the entirely nitrate-rich site of Zonal Flux (La Niña, boreal spring), we conclude that neither the ENSO nor the seasonal condition alone is responsible for the level of export. While EqPac Survey I occurred directly after the passage of a Kelvin Wave but before the ecosystem had recovered, EqPac Time-series I took place a month later, after the ecosystem had recovered. The occurrence of Tropical Instability Waves during the EqPac Survey II and Times Series II cruises was well documented. The observation of relatively high export at FLUPAC TS-II suggests that the effect of TIWs may overwhelm the effect of Kelvin waves. The low export during EqPac Survey I suggests that Kelvin Waves may be strong forcing functions. While Kelvin Waves appear to diminish export, TIWs tend to enhance it.

Within the region of persistent surface nutrients — the equatorial upwelling zone — we suggest that variability in export is a function of balance in the equatorial food web (Chavez and Barber, 1991; Landry et al., 1997), which we consider primarily a function of equatorial waves. Through this work we have developed the following working hypotheses: (1) Kelvin waves depress the food web uniformly by downwelling surface waters and decreasing the average light level experienced by phytoplankton, thus increasing grazing pressure on all phytoplankton. (2) TIWs differentially stimulate the food web by rapidly upwelling water to give an advantage to those phytoplankton that are able to quickly respond and out-compete grazing. These complex relationships between physics and biology are difficult to constrain using limited data sets, but appear to be the dominant factors determining biogeochemical fluxes in this region. Modeling of the explicit effects of Kelvin waves and TIWs on the equatorial food web and the resulting biogeochemical fluxes are the critical next step in testing these hypotheses.

Acknowledgements

We thank Robert Le Borgne, who was the chief scientist on the FLUPAC cruise and supervised the picking of swimmers, Barbara Paul for help with collection and analysis of ^{234}Th, and Jim Postel for managing the core data. We thank the entire ORSTOM-Noumea Chemistry Laboratory for their invaluable assistance in supplying us with equipment and chemicals before Zonal Flux, when our own supplies were waylaid because of a dockworkers' strike. We also thank Fanta™ for their inadvertent excellence in the production of sample bottles. As usual, the support and teamwork of the captain and crew of the R/V *Thompson* was superb. This research was supported by NASA Earth System Science Fellowship 1995-GlobalCh00307 to JPD and NSF grant 9504202 and NASA P.O. # S-67776-Z to JWM. DAH was supported by NOAA Award NA56GP0207 and NSF OCE-9311012. University of Washington, School of Oceanography Contribution Number 2214, Bermuda Biological Station for Research Contribution Number 1540 and US JGOFS Contribution Number 515.

Appendix A

Water column ^{234}Th and ^{238}U activities (dpm/l) from the FLUPAC and Zonal Flux cruises. Depth uncertainties for FLUPAC data are based on least-squares propagated uncertainties in: the beta-decay regression slope, the standard deviation of the deep ^{234}Th equilibrium calibration, the inverse square root of the alpha counts and the uncertainty in alpha counter efficiency (assumed to be 1%). Uncertainties for Zonal Flux data are based on least-squares propagated uncertainties in: the inverse square root of the beta counts, the uncertainty in beta background (high due to variable gas flow rate and ^{232}Th contamination of counters), the standard deviation of the deep ^{234}Th equilibrium calibration, the inverse square root of the alpha counts and the uncertainty in alpha counter efficiency (assumed to be 1%) (Table 6).

Table 6

Station	Latitude	Longitude	Depth (m)	U (dpm/l)	Th (dpm/l)	Uncertainty
FLUPAC						
I-1	0.0	166.8E	0–110	2.39	2.03	0.09
I-1	0.0	166.8E	110–160	2.48	2.45	0.12
I-1	0.0	166.8E	160–210	2.48	2.70	0.12
I-2	0.1N	166.6E	0–110	2.40	2.26	0.11
I-2	0.1N	166.6E	110–160	2.48	2.66	0.08
I-2	0.1N	166.6E	160–210	2.48	2.79	0.09
I-2	0.1N	166.6E	0–110	2.40	2.25	0.06
I-2	0.1N	166.6E	110–160	2.48	2.40	0.10
I-2	0.1N	166.6E	160–210	2.48	2.54	0.11
I-3	0.4N	166.5E	0–110	2.40	2.09	0.07
I-3	0.4N	166.5E	110–160	2.48	2.68	0.11
I-3	0.4N	166.5E	160–210	2.48	2.70	0.09
I-3	0.4N	166.5E	0–110	2.39	2.15	0.09
I-3	0.4N	166.5E	110–160	2.48	2.62	0.09
I-3	0.4N	166.5E	160–210	2.48	2.47	0.08
II-1	0.0	150.2W	0–100	2.47	1.82	0.08
II-1	0.0	150.2W	100–160	2.46	2.51	0.08
II-1	0.0	150.2W	160–210	2.47	2.64	0.08
II-2	0.0	150.2W	0–100	2.47	2.24	0.10
II-2	0.0	150.2W	100–160	2.47	2.60	0.12
II-2	0.0	150.2W	160–210	2.47	2.79	0.10
II-2	0.1S	149.8W	0–100	2.47	2.17	0.10
II-2	0.1S	149.8W	100–160	2.47	2.34	0.08
II-2	0.1S	149.8W	160–210	2.47	2.83	0.17
II-3	0.4S	149.5W	0–100	2.47	2.11	0.11
II-3	0.4S	149.5W	100–160	2.48	2.39	0.17

Table 6 (*continued*)

Station	Latitude	Longitude	Depth (m)	U (dpm/l)	Th (dpm/l)	Uncertainty
II-3	0.4S	149.5W	160–210	2.46	2.61	0.09
II-3	0.4S	149.5W	0–100	2.47	1.83	0.06
II-3	0.4S	149.5W	100–160	2.48	2.43	0.10
II-3	0.4S	149.5W	160–210	2.47	2.60	0.08
II-4	0.5S	149.3W	0–100	2.47	1.35	0.04
II-4	0.5S	149.3W	100–160	2.47	2.49	0.13
II-4	0.5S	149.3W	160–210	2.47	2.69	0.10
Zonal Flux						
1	2S	165E	0-140	2.50	1.77	0.20
3	0	165E	0–140	2.49	2.09	0.24
3	0	165E	140-200	2.50	2.72	0.30
6	2N	165E	0–140	2.47	2.16	0.26
6	2N	165E	140–200	2.47	2.34	0.28
7	0	170E	0–120	2.49	2.09	0.24
7	0	170E	120–200	2.50	2.06	0.28
7	0	170E	0	2.48	1.51	0.18
7	0	170E	20	2.48	1.94	0.22
7	0	170E	40	2.48	1.77	0.20
7	0	170E	80	2.48	2.06	0.26
7	0	170E	100	2.48	2.58	0.28
7	0	170E	120	2.48	2.55	0.28
7	0	170E	140	2.49	2.67	0.30
7	0	170E	160	2.48	2.55	0.30
7	0	170E	180	2.46	2.52	0.28
7	0	170E	200	2.46	2.62	0.42
8	0	175E	0–120	2.49	2.17	0.25
8	0	175E	120–200	2.50	2.40	0.26
9	0	179E	120–200	2.50	2.35	0.26
10	0	177W	0–120	2.49	2.01	0.26
11	0	171W	0–120	2.48	2.11	0.26
12	0	165W	0–120	2.48	1.84	0.26
12	0	165W	120–200	2.49	2.54	0.29
13	0	160W	0–120	2.49	1.78	0.24
13	0	160W	120–200	2.50	2.39	0.28
14	0	155W	0	2.48	1.63	0.19
14	0	155W	20	2.48	1.76	0.22
14	0	155W	40	2.48	2.15	0.28
14	0	155W	60	2.49	2.02	0.24
14	0	155W	80	2.49	2.37	0.29
14	0	155W	100	2.50	2.34	0.27
14	0	155W	140	2.49	2.56	0.29
14	0	155W	160	2.49	2.48	0.30
14	0	155W	180	2.48	2.47	0.29
14	0	155W	200	2.48	2.65	0.30
15	0	150W	0–120	2.48	2.17	0.29

Table 7

Station	Latitude (deg)	Longitude (deg)	Depth (m)	PIT mass ($mg\,m^{-2}\,d^{-1}$)	Lor. mass ($mg\,m^{-2}\,d^{-1}$)	Lor. C ($mmol\,m^{-2}\,d^{-1}$)	PIT Th ($dpm\ m^{-2}\,d^{-1}$)	Th defic. ($dpm\,m^{-2}\,d^{-1}$)	Th upwelling ($dpm\,m^{-2}\,d^{-1}$)	Th model ($dpm\,m^{-2}\,d^{-1}$)	Model C ($mmol\,m^{-2}\,d^{-1}$)
FLUPAC											
I-1	0.0	166.8E	125	540 ± 33	244 ± 39	5.53 ± 0.46	2878	1132 ± 241	233 ± 269	1366 ± 361	6.9 ± 2.9
I-2	0.1N	166.6E	120	429 ± 84	265 ± 74	4.77	1878	452 ± 307	233 ± 269	685 ± 408	6.6 ± 3.5
I-3	0.4N	166.5E	125	388 ± 48	320 ± 89	6.09 ± 0.22	2809	878 ± 266	233 ± 269	1112 ± 378	4.3 ± 2.0
II-1	0.0	150.2W	105	5990 ± 217	912 ± 67	25.6 ± 0.4	33219	1876 ± 208	875 ± 1007	2751 ± 1028	13.5 ± 6.7
II-2	0.1S	149.8W	105	3238 ± 43	1051 ± 145	20.6 ± 2.2	14513	769 ± 256	875 ± 1007	1644 ± 1039	11.7 ± 6.0
II-3	0.4S	149.5W	105	741 ± 52	1015 ± 88	24.1 ± 0.1	4081 ± 146	1428 ± 559	875 ± 1007	2302 ± 1151	11.5 ± 5.7
Zonal Flux											
1	2S	165E	140	435 ± 71	676 ± 39	9.09 ± 0.63	1890	2930 ± 800		2930 ± 800	9.1 ± 3.1
3	0.0	165E	140	690 ± 126	878 ± 75	12.1 ± 3.9	2430	1594 ± 960	934 ± 1151	2529 ± 1499	9.9 ± 7.0
6	2N	165E	140	404 ± 67	640	9.80	2565	1238 ± 1054		1238 ± 1054	3.0 ± 2.7
8	0.0	175E	120	653 ± 107	789 ± 232	12.68 ± 0.40	3840	1089 ± 871	1885 ± 2125	2974 ± 2297	8.1 ± 6.9
10	0.0	177W	120	937 ± 312	696 ± 266	11.9 ± 2.4	4234	1646 ± 886	1484 ± 1712	3131 ± 1927	11.8 ± 9.8
11	0.0	171W	120	1095 ± 89	894 ± 91	18.5 ± 4.7	7292	1298 ± 913	1421 ± 1630	2719 ± 1868	8.4 ± 6.3
13	0.0	160W	120	1807 ± 83	821 ± 3	13.4 ± 0.4	9613	2451 ± 830	1644 ± 1846	4095 ± 2024	12.6 ± 6.3
15	0.0	150W	120	976 ± 184	1321 ± 348	9.08 ± 0.62	2214	1047 ± 1006	1481 ± 1722	2528 ± 1995	7.7 ± 6.6

Appendix B

Sediment Trap mass carbon and ^{234}Th data and ^{234}Th model results from the FLUPAC and Zonal Flux cruises. Confidence intervals for sediment trap data are standard deviations of replicates. Confidence intervals for ^{234}Th model results are based on least-squares propagated uncertainties. In cases where no replicates were available to determine sediment trap uncertainties, average fractional uncertainties were used (Table 7).

References

Anderson, R.F., Fleer, A.P., 1982. Determination of natural activities of thorium and plutonium in marine particle material. Analytical Chemistry 54, 1142–1147.

Archer, D., Peltzer, E.T., Kirchman, D., 1997a. A timescale for dissolved organic carbon production in equatorial Pacific surface waters. Global Biogeochemical Cycles 11, 435–452.

Archer, D. et al., 1997b. Shipboard observations of a convergent front at 2°N during JGOFS Survey II Expedition in August, 1992. Deep-Sea Research Part II 44, 1827–1849.

Aufdenkampe, A.K., McCarthy, J.J., Dunne, J.P., Rodier, M., Murray, J.W., New production along the equator in the central Pacific. Deep-Sea Research, submitted.

Bacon, M.P., Cochran, J.K., Hirshberg, D., Hammar, T.R., Fleer, A.P., 1996. Export fluxes of carbon at the equator during the EqPac time-series cruises estimated from ^{234}Th measurements. Deep-Sea Research II 43, 1133–1154.

Barber, R.T., Kogelschatz, J.E., 1990. Nutrients and productivity during the 1982/83 El Niño. In: Glynn, P.W. (Ed.), Global Consequences of the 1982/83 El Niño-Southern Oscillation Event. Elsevier, Amsterdam.

Barber, R.T., Chavez, F.P., 1991. Regulation of primary productivity rate in the equatorial Pacific. Limnology and Oceanography 36, 1803–1815.

Barber, R.T., Sanderson, M.P., Lindley, S.T., Chai, F., Newton, J., Trees, C.C., Foley, D.G., Chavez, F.P., 1996. Primary productivity and its regulation in the equatorial Pacific during and following the 1991–1992 El Niño. Deep-Sea Research II 43, 933–969.

Bidigare, R.R., Ondrusek, M.E., 1996. Spatial and temporal variability of phytoplankton pigment distributions in the central equatorial Pacific Ocean. Deep-Sea Research II 43, 809–834.

Buesseler, K.O., Bacon, M., Cochran, J.K., Livingston, H., 1992. Carbon and nitrogen export during the JGOFS North Atlantic Bloom Experiment estimated from ^{234}Th : ^{238}U disequilibria. Deep-Sea Research 39, 1115–1137.

Buesseler, K.O., Michaels, A.F., Siegel, D.A., Knap, A.H., 1994. A three dimensional time-dependent approach to calibrating sediment trap fluxes. Global Biogeochemical Cycles 8, 179–193.

Buesseler, K.O., Andrews, J., Hartman, M., Belastock, R., Chai, F., 1995. Regional estimates of the export flux of particulate organic carbon derived from thorium-234 during the JGOFS EQPAC program. Deep-Sea Research II 42, 777–804.

Chai, F., 1995. Origin and Maintenance of High Nitrate Condition in the Equatorial Pacific, a biological-physical model study. Ph.D. Dissertation, Duke University, Durham, NC, 170 pp.

Charette, M.A., Moran, S.B., Bishop, J.K.B., 1999. ^{234}Th as a tracer of particulate organic carbon export in the subarctic northeast Pacific Ocean. Deep-Sea Research II 46, 2833–2861.

Chavez, F.P., Barber, R.T., 1987. An estimate of new production in the equatorial Pacific. Deep-Sea Research 34, 1229–1243.

Chavez, F.P., Toggweiler, J.R., 1995. Physical estimates of global new production: the upwelling contribution. In: Summerhayes, Emeis, Angel, Smith, Zeitschel, (Eds.), Upwelling in the Ocean: Modern Processes and Ancient Records. Wiley, New York.

Chavez, F.P., Strutton, P.G., McPhaden, M.J., 1998. Biological-physical coupling in the central equatorial Pacific during the onset of the 1997–98 El Niño. Geophysical Research Letters 25, 3543–3546.

Chen, J.H., Edwards, R.L., Wasserburg, G.J., 1986. ^{238}U, ^{234}U and ^{232}Th in seawater. Earth and Planetary Science Letters 80, 241–251.

Coale, K.H., Bruland, K.W., 1985. ^{234}Th : ^{238}U disequilibria within the California Current. Limnology and Oceanography 30, 22–33.

Dunne, J., 1999. Measured and modeled particle export in equatorial and coastal upwelling regions. Ph.D. Dissertation, University of Washington, Seattle, WA, 167 pp.

Dunne, J.P., Murray, J.W., Young, J., Balistrien, L.S., Bishop, J., 1997. ^{234}Th and particle cycling in the central equatorial Pacific. Deep-Sea Research II 44, 2049–2083.

Dunne, J.P., Murray, J.W., 1999a. Sensitivity of ^{234}Th export to physical processes in the central equatorial Pacific. Deep-Sea Research I 46, 831–854.

Dunne, J.P., Murray, J.W., Aufdenkampe, A., Rodier, M., 1999b. Silicon-nitrogen coupling in the equatorial Pacific upwelling zone. Global Biogeochemical Cycles 13, 715–726.

Eldin, G., Rodier, M., Radenac, M.-H., 1997. Physical and nutrient variability in the upper equatorial Pacific associated with westerly wind forcing and wave activity in October 1994. Deep-Sea Research II 44, 1783–1800.

Emerson, S., Quay, P., Karl, D., Winn, C., Tupas, L., Landry, M., 1997. Experimental determination of organic carbon flux from open-ocean waters. Nature 389, 951–954.

Flament, P.J., Kennan, S.C., Knox, R.A., Niiler, P.P., Bernstein, R.L., 1996. The three-dimensional structure of an upper ocean vortex in the tropical Pacific ocean. Nature 383, 610–613.

Foley, D.G., Dickey, T.D., McPhaden, M.J., Bidigare, R.R., Lewis, M.R., Barber, R.T., Lindley, S.T., Garside, C., Manov, D.V., McNeil, J.D., 1997. Longwaves and primary productivity variations in the equatorial Pacific at 0°, 140°W. Deep-Sea Research 44, 1801–1826.

Hansell, D.A., Bates, N., Carlson, C.A., 1997a. Predominance of vertical loss of carbon from surface waters of the equatorial Pacific Ocean. Nature 386, 59–61.

Hansell, D.A., Carlson, C.A., Bates, N.A., Poisson, A., 1997b. Horizontal and vertical removal of organic carbon in the equatorial Pacific Ocean: a mass balance assessment. Deep-Sea Research II 44, 2115–2130.

Harrison, D.E., 1996. Vertical velocity in the central equatorial Pacific: a circulation model perspective for JGOFS. Deep-Sea Research II 43, 687–705.

Karl, D.M., Christian, J.R., Dore, J.E., Hebel, D.V., Letelier, R.M., Tupas, L.M., Winn, C.D., 1996. Seasonal and interannual variability in primary production and particle flux at station ALOHA. Deep-Sea Research II 43, 539–568.

Kessler, W.S., McPhaden, M.J., 1995. The 1991–1993 El Niño in the central Pacific. Deep-Sea Research II 42, 295–334.

Knauer, G.A., Martin, J.H., Bruland, K.W., 1979. Fluxes of particulate carbon, nitrogen and phosphorous in the upper water column of the northeast Pacific. Deep-Sea Research 26, 97–108.

Ku, T.-L., Knauss, K.G., Matieu, G.G., 1977. Uranium in open ocean: concentration and isotopic composition. Deep-Sea Research 24, 1005–1017.

Landry, M.R., Constantinou, J., Kirshtein, J., 1995. Microzooplankton grazing in the central equatorial Pacific during February and August, 1992. Deep-Sea Research II 42, 657–672.

Landry, M.R., et al. 1997. Iron and grazing constraints on primary production in the central equatorial Pacific: an EqPac synthesis. Limnology and Oceanography 42, 405–418.

Le Borgne, R., Rodier, M., LeBouteiller, A., Murray, J.W., 1999. Zonal variability of biological features and particle export flux in the pacific equatorial upwelling between 165°E and 150°W (April–May, 1996). Oceanologica Acta 22, 57–66.

Le Borgne, R., Brunet, C., Eldin, G., Radenac, M.-H., Rodier, M., 1995. Campagne Oceanographique FLUPAC a bord du N.O. l'atalante (23 septembre au 29 octobre 1994). Recueil des donnees. Tome 1: meteo, courantologie, hyrologie, donnees de surface. ORSTOM. Noumea Archives Sciences de la Mer, Oceanographique 1, 1–340.

Le Borgne, R., Gesbert, H., 1995. Campagne Oceanographique FLUPAC a bord du N.O. l'atalante (23 septembre au 29 octobre 1994). Recueil des donnees. Tome 2: optique marine, matiere organic dissoute, pigments photosynthetiques, observations microscopiques, production primaire, "broutage", zooplancton, sedimentation. ORSTOM. Noumea Archives Sciences de la Mer, Oceanographique 2, 1–303.

Lorenzen, C.J., Welschmeyer, N.A., Copping, A.E., Vernet, M., 1983. Sinking rates of organic particles. Limnology and Oceanography 28, 766–769.

Loukos, H., Frost, B., Harrison, D.E., Murray, J.W., 1997. Ecosystem model with iron limitation of primary production in the equatorial Pacific at 140°W. Deep-Sea Research II 44, 2221–2249.

Mackey, D.J., Parslow, J.S., Griffiths, F.B., Higgins, H.W., Tillbrook, B., 1997. Phytoplankton productivity and the carbon cycle in the western equatorial Pacific under El Niño and non-El Niño conditions. Deep-Sea Research II 44, 1951–1978.

McCarthy, J.J., Garside, C., Nevins, J.L., Barber, R.T., 1996. New production along 140°W in the equatorial Pacific during and following the 1992 El Niño event. Deep-Sea Research II 43, 1065–1093.

Michaels, A.F., Bates, N.R., Buesseler, K.O., Carlson, C.A., Knap, A.H., 1994. Carbon-cycle imbalances in the Sargasso Sea. Nature 372, 537–540.

Murray, J.W., Barber, R.T., Roman, M.R., Bacon, M.P., Feely, R.A., 1994. Physical and biological controls on carbon cycling in the equatorial Pacific. Science 266, 58–65.

Murray, J.W., Young, J., Newton, J., Dunne, J., Chapin, T., Paul, B., McCarthy, J.J., 1996. Export flux of particulate organic carbon from the central equatorial Pacific determined using a combined drifting trap-^{234}Th approach. Deep-Sea Research II 43, 1095–1132.

Philander, S.G., 1990. In: Dmowska, R., Holton, J.R. (Eds.), El Niño, La Niña, and the Southern Oscillation. Academic Press, New York.

Quay, P., 1997. Was a carbon balance measured in the equatorial Pacific during JGOFS? Deep-Sea Research II 44, 1765–1781.

Rodier, M., Le Borgne, R., 1997. Export flux of particles at the equator in the western and central Pacific Ocean. Deep-Sea Research II 44, 2085–2113.

Sokal, R.R., Rohlf, F.J., 1995. Biometry: the Principles and Practice of Statistics in Biological Research. W. H. Freeman and Company, SanFrancisco, CA.

Yoder, J.A., Ackleson, S.G., Barber, R.T., Flament, P., Balch, W.M., 1994. A line in the sea. Nature 371, 689–692.